

# **HYALURONIC ACID-BASED HYDROGELS FOR CARTILAGE REPAIR**

by

Xinyi Wang

A thesis submitted to the Faculty of the University of Delaware in partial fulfillment of the requirements for the degree of Master of Science in Materials Science and Engineering

Summer 2012

Copyright 2012 Xinyi Wang  
All Rights Reserved

# HYALURONIC ACID-BASED HYDROGELS FOR CARTILAGE REPAIR

by

Xinyi Wang

Approved: \_\_\_\_\_

Xinqiao Jia, Ph.D.

Professor in charge of thesis on behalf of the Advisory Committee

Approved: \_\_\_\_\_

David C. Martin, Ph.D.

Chair of the Department of Materials Science and Engineering

Approved: \_\_\_\_\_

Babatunde Ogunnaike, Ph.D.

Interim Dean of the College of Engineering

Approved: \_\_\_\_\_

Charles G Riordan, Ph.D.

Vice Provost for Graduate and Professional Education

## ACKNOWLEDGMENTS

I am deeply indebted to all the people who supported me and encouraged me to complete this thesis work. It is my pleasure to pay tribute to them in this section.

Foremost, I would like to express my sincere gratitude to my advisor, Professor Xinqiao Jia, for her support, guidance and encouragement on my lab work, which proactively helped me gain much knowledge about biomaterials. Productive scientific discussions with her significantly increased my knowledge and expertise for conducting experiments. This work would not have been accomplished without her enthusiasm and encouragement, and thus I would like to sincerely acknowledge all of her efforts to make me an independent researcher.

I am grateful to Professor Anja Nohe from the Department of Biological Sciences at the University of Delaware and Professor Rodney Clifton from Brown University for their intellectual input, collaborative efforts and guidance. The communications with their teams helped expand my knowledge in biological and mechanical fields, which facilitates my academic success.

I would also like to acknowledge my fellow lab mates for their help, support and suggestions throughout my Master's thesis. Furthermore, I would like to thank all staff (especially Charlie Garbini, Christine Williamson, Dionne Putney, and Diane Clark) in the Department of Material Science and Engineering for helping me with administrative work and providing safety guidance for maintaining a safe working environment. I am thankful to Dr. Kirk Czymmek, Dr. Jeffrey Caplan, Dr. Chaoying Ni and Mr. Frank Kriss for being available to help me use the microscopy facilities, which had been instrumental in my thesis work. I would like to thank all my friends for being available to help me, providing encouragement and fun outside the laboratory.

Last but not least, I am thankful to my parents for their unconditional love, support, care and encouragement.

## TABLE OF CONTENTS

LIST OF TABLES.....	viii
LIST OF FIGURES.....	ix
ABSTRACT.....	xi

### Chapter

1 INTRODUCTION.....	1
1.1 Cartilage Anatomy and Osteoarthritis.....	1
1.2 HA-based Hydrogels.....	2
1.3 Thesis Summary.....	4
REFERENCES.....	6
2 HA-BASED, PEPTIDE-RELEASING HYDROGEL PARTICLES.....	7
2.1 Introduction.....	7
2.2 Materials and Methods.....	9
2.2.1 Materials.....	9
2.2.2 Synthesis of $\alpha$ -hydroxyl, $\omega$ -acrylate oligomeric lactic acid (HEALA-OH).....	9
2.2.3 Synthesis of $\alpha$ -carboxylate, $\omega$ -acrylate oligomeric lactic acid (HEALA-COOH).....	10
2.2.4 Synthesis of NHS Activated Lactic Acid Oligomers (HEALA-NHS).....	10
2.2.5 Synthesis of HEALA-Modified HA HGPs (HEALA-HGPs).....	11
2.2.6 Synthesis of CK2.1 Modified HA HGPs (CK2.1-HGPs).....	11
2.2.7 In vitro Peptide Release.....	12
2.3 Results and Discussion.....	12
2.3.1 Synthesis of Degradable Linkers.....	12
2.3.2 Synthesis of HEALA-HGPs.....	17
2.3.3 Peptide Conjugation and Release.....	19
2.4 Conclusion.....	21
REFERENCES.....	22

3	CHONDROGENIC DIFFERENTIATION OF MESENCHYMAL STEM CELLS CULTURED IN HYALURONIC ACID-BASED DOUBLY CROSSLINKED NETWORKS .....	24
3.1	Introduction .....	24
3.2	Materials and Methods .....	27
3.2.1	Materials .....	27
3.2.2	Synthesis of Glycidal Methacrylate-modified HA (HAGMA).....	28
3.2.3	Synthesis of Gelatin-Conjugated HA HGPs .....	29
3.2.3.1	Preparation of HA HGPs .....	29
3.2.3.2	Synthesis of Gelatin-conjugated HA-based Hydrogel Particles (HA gHGPs) .....	29
3.2.3.3	Evaluation of Gelatin Conjugation .....	30
3.2.3.4	Particle Size Analysis .....	30
3.2.4	MSC Culture in HADXNs .....	31
3.2.5	Cell Viability and Proliferation.....	32
3.2.6	Cell Morphology and Focal Adhesion.....	33
3.2.7	Cell Differentiation.....	34
3.2.7.1	Chondrogenesis.....	34
3.2.7.2	Osteogenesis and Adipogenesis .....	35
3.2.8	Hydrogel Mechanical Properties .....	36
3.2.8.1	Traditional Rheological Characterization.....	36
3.2.8.2	TWA Characterization .....	36
3.2.9	Statistical Analysis .....	37
3.3	Results and Discussion.....	37
3.3.1	Synthesis of HAGMA.....	37
3.3.2	Synthesis and Characterization of HA gHGPs .....	38
3.3.3	Cell Viability and Proliferation.....	39
3.3.4	Cell Morphology and Focal Adhesion.....	44
3.3.5	Cell Differentiation.....	45
3.3.6	Viscoelastic Properties of the Cell/gel Constructs .....	53
3.4	Conclusion.....	58
	REFERENCES .....	59

Appendix

PERMISSION LETTERS.....61

## LIST OF TABLES

<b>Table 3.1</b>	Viscoelastic properties of HA hydrogels and cell/gel constructs assessed by commercial rheometer at frequencies of 01-10 Hz and TWA at frequencies of 10-100 Hz.....	58
------------------	--	----

## LIST OF FIGURES

<b>Figure 1.1</b>	Human knee. (a) Example MR image of a knee joint—femur, patella, and tibia bones with associated cartilage surfaces are clearly visible. FB=femoral bone, TB=tibial bone, PB=patellar bone, FC=femoral cartilage, TC=tibial cartilage, PC=patellar cartilage. (b) Schematic view of knee anatomy.....	1
<b>Figure 2.1</b>	Covalent immobilization of CK2.1 peptide to HA HGPs through a hydrolytically degradable linker.....	8
<b>Figure 2.2</b>	<sup>1</sup> H NMR spectrum of HEALA-OH. Solvent: CDCl <sub>3</sub> .....	14
<b>Figure 2.3</b>	<sup>1</sup> H NMR spectrum of HEALA-COOH. Solvent: CDCl <sub>3</sub> .....	15
<b>Figure 2.4</b>	<sup>1</sup> H NMR spectrum of HEALA-NHS. Solvent: CDCl <sub>3</sub> .....	16
<b>Figure 2.5</b>	Reaction scheme for the synthesis of HEALA-HGPs .....	17
<b>Figure 2.6</b>	<sup>1</sup> H NMR spectrum of acrylate modified particles after degradation .....	18
<b>Figure 2.7</b>	Peptide standard curve obtained at 280nm .....	19
<b>Figure 2.8</b>	Peptide release curve obtained at 280nm.....	20
<b>Figure 3.1</b>	Fabrication of three types of cell-seeded gels: the HAGMA-gHGP gel, the HAGMA-HGP gel and the HAGMA gel .....	31
<b>Figure 3.2</b>	<sup>1</sup> H NMR spectrum of HAGMA. Solvent: D2O .....	38
<b>Figure 3.3</b>	(A)Fluorescamine staining of gelatin conjugated HA HGPs (left) and unmodified HA HGPs (right); (B) Particle size distribution measured by coulter counter; Mean size: 6-7 μm. Three repeating samples were used for each type of particles.....	39

<b>Figure 3.4</b>	Cell proliferation measured by the Alamar Blue assay during 35 days of culture in gels (normalized to the original cell-seeding number). * indicates cell number was statistically significantly different from that at the previous time point, $p < 0.05$ . # indicates cell number was statistically significantly different from that in HAGMA gels at the same day, $p < 0.05$ .....	41
<b>Figure 3.5</b>	Live/dead staining of cells (A-F) after 10 days, (G-L) after 20 days and (M-R) after 30 days of hMSC culture in gels. (A-C,G-I,M-O): Top view projection of all z-series sections. (D-F,J-L,P-R): Side view projection of all z-series sections. Live cells were stained green while dead cells were stained red... ..	42
<b>Figure 3.6</b>	Immunostaining of MSCs after 15 days of culture in HA gels. (A-L) One slide view for gels: (A-C) nuclei staining with DAPI (blue); (D-F) F-actin staining with rhodamine phalloidin (red); (G-I) integrin staining with primary anti-integrin $\alpha_2 \beta_1$ antibody and Alexa Fluor 488 goat anti-mouse antibody (green) (J-L) Overlay of staining in three channels and particles in phase contrast mode. (M-O) Top view projection of all z-series sections for gels.....	44
<b>Figure 3.7</b>	Immunostaining of (A) collagen II and aggrecan (Z-stack projection and one slide comparison), (B) collagen II, (C) aggrecan and (D) blank controls and negative controls for collagen II and aggrecan staining. (A): All cells had stained F-actin and nuclei as reference. (B), (C): projection of a Z-stack reconstruction image of cells after 10, 20, 25 and 30 days of MSC culture in three types of gels.....	49
<b>Figure 3.8</b>	Histological staining of GAGs with Alcian Blue for (A) MSCs (B) differentiated cells after 30 days of culture in three random areas of gels after cryostat sectioning. Scare bar: 50 $\mu\text{m}$ .....	52
<b>Figure 3.9</b>	Staining of (A-C) lipids with Oil Red O, (D-F) calcium with Alizarin Red S and (G-I) Collagen I with antibodies for cells after 30 days of MSC culture in gels. Scare bar: 50 $\mu\text{m}$ . .....	53
<b>Figure 3.10</b>	The frequency dependence of the storage (solid symbols) and loss (open symbols) moduli on 0.1% strain for (A) cell-free HA based gels and (B) cell-seeded HA based gels at lower frequency; three repeating samples were used for each type of gels. Cell-seeded gels were removed after 30 days of MSC culture .....	56

**Figure 3.11** Frequency dependence of amplification factors for (A) cell-free HA based gels and (B) cell seeded gels. The viscoelastic moduli that provide the best fit between model predictions (curves) and experimental results (symbols) for the respective materials were measured. Each experiment was conducted with three repeats.....57

## ABSTRACT

We are interested in developing hyaluronic acid (HA)-based hydrogels that can be used for cartilage repair and regeneration. To this end, nanoporous HA hydrogel particles (HGPs) with an average diameter of 6-7  $\mu\text{m}$  were synthesized in an inverse water-in-oil emulsion system. A synthetic peptide, CK2.1, with chondro-inductive potentials, was covalently conjugated to HA HGPs via a hydrolytically degradable linker and was released from HGPs in controlled manner over 7 days. Alternatively, reductive amination reaction was employed for covalent immobilization of gelatin to HGPs (gHGPs). Separately, glycidyl methacrylate was allowed to react with HA to yield HA-glycidyl methacrylate (HAGMA) conjugates. HA-based doubly crosslinked network hydrogels (DXNs) were synthesized via UV-initiated radical crosslinking of HAGMA macromonomers in the presence of HGPs. When gHGPs were used in place of HGPs, cell-adhesive HA DXNs were obtained. Human mesenchymal stem cells (hMSCs) entrapped in HAGMA-gHGP gels were able to attach to the matrix through focal adhesion. The cell-adhesive HA DXNs induced the chondrogenic differentiation of hMSCs in MSC maintenance media, as evidenced by the expression of cartilage-specific matrix components (eg collagen II, aggrecan and sulfated glycosaminoglycan, sGAG). The viscoelastic properties of HA DXNs were assessed at low frequencies (<10 Hz) by a commercial rheometer and at high frequencies (10-100 Hz) using a home-built torsional wave apparatus (TWA). Compared to the cell-free DXNs, the

cell/gel constructs were stiffer. The  $G'$  value of cell-seeded HAGMA-gHGP gels were  $1210 \pm 70$  Pa and  $1502 \pm 220$  Pa at frequencies of 0.1-10 Hz and around 50 Hz, respectively.

## Chapter 1

### INTRODUCTION

#### 1.1. Cartilage Anatomy and Osteoarthritis

Articular cartilage is a connective tissue that lines the articular surface of bones at diarthrodial joints. It is an avascular and aneural tissue, serving as a cushion and providing mechanical support. Articular cartilage is generally divided into four zones based on the morphological and histological characteristics the superficial zone, the transitional zone, the deep zone, and the calcified zone. Although the tissue composition differs structurally through each of these zones, articular cartilage is primarily composed of type II collagen, proteoglycans, and small amounts of other non-collagenous proteins, as well as sulfated glycosaminoglycans. The primary type of cells within the tissue is chondrocytes, which produce and maintain the cartilage matrix<sup>1</sup>.

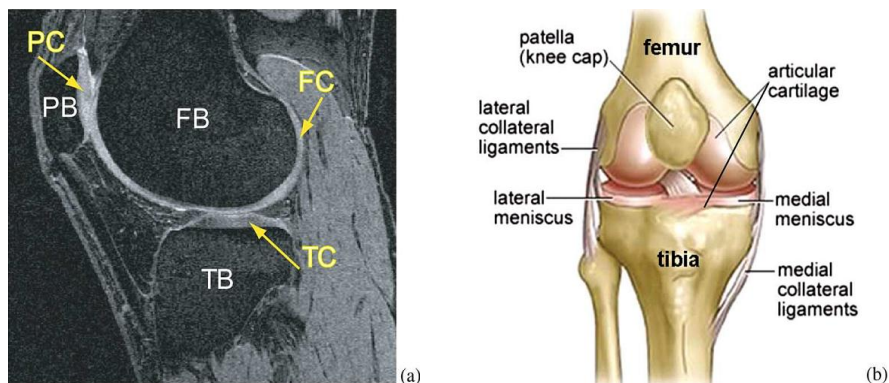


**Figure 1.1** Human knee. (a) Example MR image of a knee joint—femur, patella, and tibia bones with associated cartilage surfaces are clearly visible. FB = femoral bone, TB = tibial bone, PB = patellar bone, FC = femoral cartilage, TC = tibial cartilage, PC = patellar cartilage. (b) Schematic view of knee anatomy<sup>2</sup>

Osteoarthritis (OA) is a term given to a group of mechanical abnormalities that is characterized by the thinning or degradation of articular cartilage and the underlying bone. OA affects almost 27 million Americans and costs the U.S. economy over \$128 billion every year, and this significant percentage of the population presents with pain and stiffness of joints that lead to decreased productivity and decreased life quality<sup>3</sup>. The increasing population of younger patients due to sports injuries has resulted in a much worse situation. These individuals require lifelong treatment and are more difficult to manage, as more active persons are likely to inflict more damage to already weakened cartilage tissues. If left untreated, the articular cartilage will degrade over time, leading to the remodeling of subchondral bone, joint pain, and loss of flexibility. The damaged cartilage lacks the ability for self-repair<sup>4-5</sup>. Therefore, the development of bioactive hydrogels for cartilage repair and regeneration is the focus of my thesis.

## **1.2. HA-Based Hydrogels**

Hyaluronic acid (HA) is a ubiquitous non-sulfated glycosaminoglycan (GAG) present throughout all extracellular matrices (ECM) in vertebrates<sup>6</sup>. HA is biocompatible, biodegradable, anti-inflammatory, non-immunogenic, and non-thrombogenic. In cartilage, HA binds aggrecan to form large aggregates within the collagenous framework, providing compressive resistance to the tissue. Cellular interactions between chondrocytes and HA help organize the cartilage ECM and retain the proteoglycans within the cartilage. Thus, HA is an attractive for use in cartilage repair. However, natural HA is not a useful biomaterial because dissolution of HA in aqueous media gives rise to a viscous liquid

without any mechanical integrity<sup>7</sup>. Moreover, natural HA can be easily degraded by hyaluronidase. Chemical modification and covalent crosslinking help stabilize HA and improve its mechanical properties. Our group has previously developed several methods for the introduction of different functionalities, such as methacrylate groups<sup>8</sup>, hydrazide groups<sup>9</sup> and aldehyde groups<sup>9</sup>, to HA. These reactions occur under mild conditions and do not alter the biological properties of HA significantly. These chemistries have been utilized for the production of macroscopic gels and microscopic hydrogel particles (HGPs)<sup>10</sup>.

Jia et al. reported the synthesis and fabrication of HA HGPs with an average diameter of 10  $\mu\text{m}$  in 2006<sup>10</sup>. First, chemically modified HA derivatives with complementary reactive groups, aldehyde groups, and hydrazide groups were prepared. Specifically, sodium periodate oxidation of HA gave rise to aldehyde-containing HA (HAALD). Separately, carbodiimide-mediated coupling reaction between HA and adipic acid dihydrazide (ADH) afforded hydrazide-carrying HA (HAADH). HA HGPs were prepared by crosslinking HAALD and HAADH in a water-in-oil inverse emulsion system stabilized by Span 80<sup>10</sup>. These nanoporous HA HGPs are ideal depots for the sequestration and release of growth factors<sup>11-12</sup>. Perlecan domain I (PInDI), a module of a basement membrane proteoglycan with a strong affinity for heparin binding growth factors (HBGFs), was conjugated to the particles via a flexible poly (ethylene glycol) (PEG) linker<sup>11</sup>. The immobilized PInDI maintains its ability to bind BMP-2, modulating its release and potentiating its biological functions<sup>12</sup>. Using a micromass culture format, we showed that the released BMP-2 effectively induced the chondrogenic differentiation of hMSCs.

The Jia Group has also prepared HA-based doubly crosslinked networks (DXNs) consisting of HA HGPs physically entrapped or covalently integrated in a secondary network that is also HA-based<sup>13</sup>. For example, UV-imitated radical crosslinking of HAGMA in the presence of methacrylated HA HGPs resulted in HA DXNs that not only foster the proliferation of primary bovine chondrocytes but also facilitate the production of cartilage-specific matrix components<sup>14</sup>. To improve cell adhesion to HA DXNs, gelatin was covalently immobilized to HGPs via a reductive amination reaction between the aldehyde groups of HA HGPs and the lysine amines of gelatin, and the gelatin conjugated particles are referred to as gHGPs. Cell-adhesive HA DXNs were prepared by entrapping gHGPs in HAGMA networks. hMSCs seeded on the gels readily attached to the matrix through the adhesive sites clustered at the particle surfaces. After prolonged culture of hMSC on the hydrogels, hMSCs were differentiated into osteoblasts in the absence of soluble osteogenic factors in the culture media<sup>15</sup>.

### **1.3. Thesis Summary**

Built upon the pioneering work described above, I have conducted investigations to evaluate the utility of HA HGPs and DXNs for cartilage repair. In **Chapter 2**, I describe our effort in developing a delivery system for a peptide, CK2.1, which has been shown to stimulate the chondrogenic differentiation of cultured hMSCs. Specifically, the CK2.1 peptide was covalently conjugated to HA HGPs via a thiol-ether linkage with neighboring ester groups, and thus the release of CK2.1 was controlled by the hydrolysis of ester groups. During 7 days of release, peptide was slowly released from particles in a controlled fashion at pH 7.4 at 37

°C. In **Chapter 3**, I describe the ability of cell-adhesive HA DXNs to coax hMSCs to undergo chondrogenic differentiation in three-dimensional (3D) scaffolds. Cell-adhesive HA DXNs were prepared by entrapping HA gHGs in a photocrosslinkable secondary matrix. Cells attached to HA gHGs through the adhesive sites on particle surfaces. Cells cultured in 3D matrices did not proliferate as readily as those plated on 2D TCPS. They did not adopt the classical spread-out morphology as those seen on 2D cultures either. However, hMSCs in HAGMA-gHGP gels developed distinct focal adhesions and produced cartilage-specific ECM components. The viscoelastic properties of HA DXNs were subsequently analyzed by rheometry and torsional wave analysis at various frequencies.

## REFERENCES

- [1] Huber, M.; Trattnig, S.; Lintner, F. *Investigative Radiology* **2000**, *35*,573-580.
- [2] Yin, Y.; Zhang, X.; Williams, R.; Wu, X.; Anderson, D. D.; Sonka, M. *IEEE Transactions on Medical Imaging* **2010**, *29*, 2023-2037.
- [3] Hunter, D. J.; Lo, G. H. *Medical Clinics of North America* **2009**, *93*,127-143.
- [4] Place, E. S.; Evans, N. D.; Stevens, M. M. *Nature Materials* **2009**, *8*, 457-470.
- [5] Chen, W. Y. J. and Abatangelo, G. *Wound Repair and Regeneration* **1999**, *7*, 79–89.
- [6] Garg, H.G.; Hales, C. A. *Chemistry and Biology of Hyaluronan*. Elsevier Ltd.; Oxford: **2004**.
- [7] Laurent, T. C. E. *The Chemistry, Biology, and Medical Applications of Hyaluronan and Its Derivatives*. Portland Press; Miami: **1998**.
- [8] Jia, X.; Burdick, J. A.; Kobler, J.; Clifton, R. J.; Rosowski, J. J.; Zeitels, S. M.; Langer, R. *Macromolecules* **2004**, *37*, 3239-3248.
- [9] Jia, X.; Colombo, G.; Padera, R.; Langer, R.; Kohane, D. S. *Biomaterials* **2004**, *25*, 4797-4804.
- [10] Jia, X.; Yeo, Y.; Clifton, R. J.; Jiao, T.; Kohane, D. S.; Kobler, J. B.; Zeitels, S. M.; Langer, R. *Biomacromolecules* **2006**, *7*, 3336-3344.
- [11] Xu, X.; Jha, A. K.; Duncan, R. L.; Jia, X. *Acta Biomaterialia* **2011**, *7*, 3050-3059.
- [12] Jha, A. K.; Yang, W.; Kirn-Safarn, C. B.; Farach-Carson, M. C.; Jia, X. *Biomaterials* **2009**, *30*, 6964-6974.
- [13] Jha, A. K.; Hule, R.A.; Jiao, T.; Teller, S.; Clifton, R. J.; Duncan, R. L.; Pochan, D. J.; Jia, X. *Macromolecules* **2009**, *42*, 537-546.
- [14] Jha, A. K.; Malik, M. S.; Farach-Carson, M. C.; Duncan, R. L.; Jia, X. *Soft Matter* **2010**, *6*, 5045-5055.
- [15] Jha, A. K.; Xu, X.; Duncan, R. L.; Jia, X. *Biomaterials* **2011**, *32*, 2466-2478.

## Chapter 2

### HA-BASED, PEPTIDE-RELEASING HYDROGEL PARTICLES

#### 2.1. Introduction

Bone morphogenetic proteins (BMPs) play a crucial role during embryonic development and regulate processes such as neurogenesis, chondrogenesis and hematopoiesis. Upon binding of BMP receptors, several signaling pathways, including Smad and p38, are activated. BMP-2 is proven to induce chondrogenic differentiation in hMSCs, increasing chondrocyte proliferation. However, BMP-2 helps stimulate osteogenesis and induces apoptosis in chondrocytes and osteoblasts<sup>1-3</sup>. To overcome such shortcoming, CK2.1 was developed to regulate the BMP-2 signaling downstream of BMPRIa<sup>4</sup>. To maximize the therapeutic potential of this peptide, injectable hydrogel particles with controlled release capacity for CK2.1 were developed. In this chapter, HA-based HGPs was used as drug carriers to improve the bioavailability and enzymatic stability of CK2.1<sup>6-7</sup>. HA was chosen as the starting material due to its biocompatibility and biodegradability. In addition, HA, which was abundant in human cartilage where cellular interactions between chondrocytes, helped organize the cartilage extracellular matrices (ECM) and retain the proteoglycans<sup>5</sup>.

This chapter describes the covalent immobilization of CK2.1 peptide to HA HGPs. The basic peptide sequence of CK2.1 is RQIKIWFQNRRMKWKKMVPSPSYEDM. A cyste-

ine residue was introduced to the C-terminus via a glycine linker. The cysteine-tagged CK2.1 was covalently conjugated to acrylated HA HGPs via a oligomeric lactic acid linker through a Michael addition reaction (Figure 2.1) and the CK2.1 release rate was controlled by the hydrolysis rate of the ester groups<sup>8, 10</sup>.

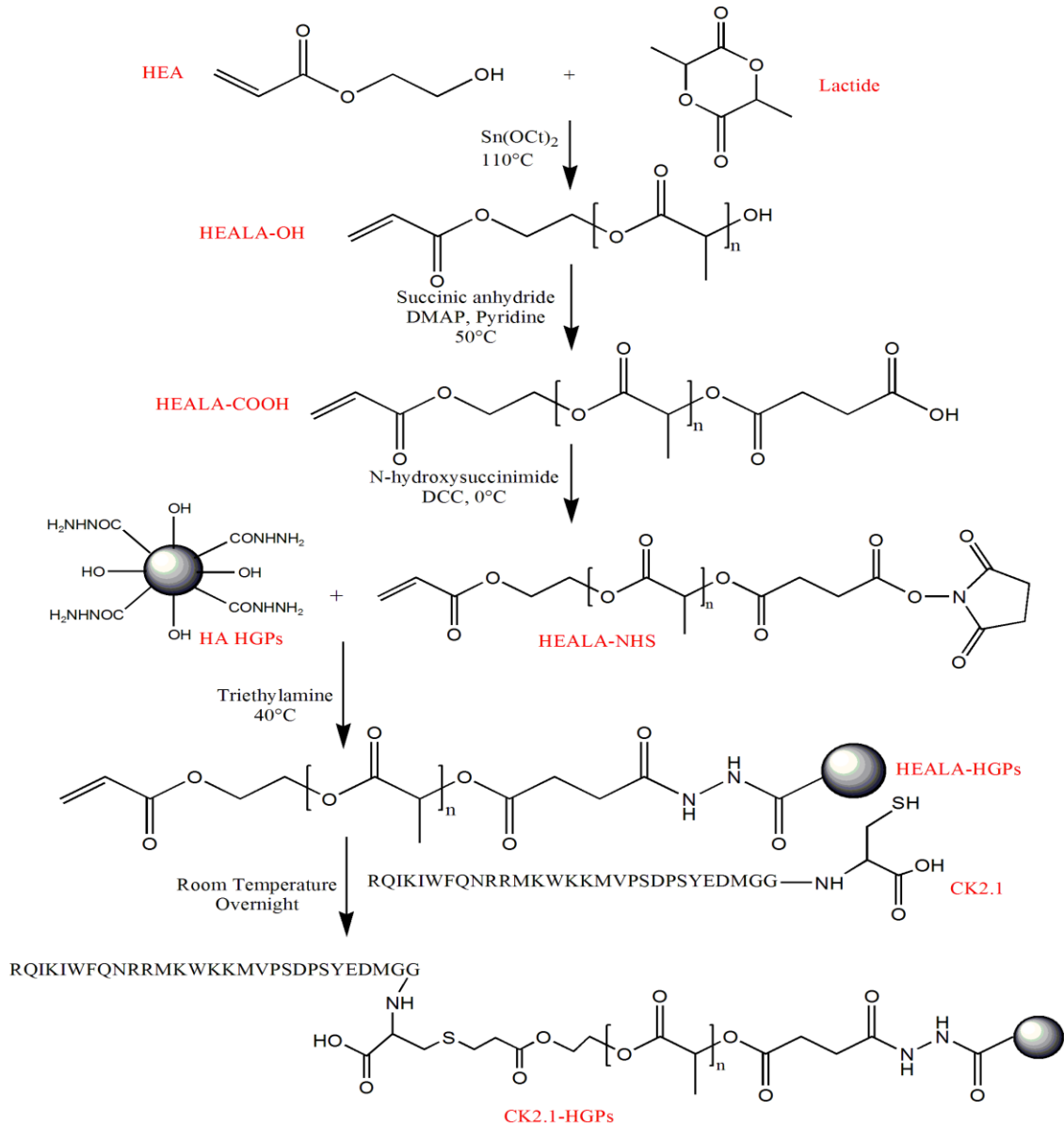


**Figure 2.1** Covalent immobilization of CK2.1 peptide to HA HGPs through a hydrolytically degradable linker.

## 2.2. Materials and Methods

### 2.2.1. Materials

Hyaluronic acid (HA, sodium salt, 500 kDa) was a gift from Genzyme Corporation (Cambridge, MA, USA). The basic CK2.1 peptide sequence RQIKIWFQNRRKWKKMV-PSDPSYEDM with a molecular weight of 3499.12 Da and cysteine-tagged CK2.1 sequence RQIKIWFQNRRKWKKMVPSDPSYEDMGGC with a molecular weight of 3716.36 Da were purchased from GenScript (Customer Peptide Synthesis). Hydroxyethyl acrylate (HEA), lactide, stannous octoate ( $\text{Sn}(\text{Oct})_2$ ), hydroquinone, naphthalene, potassium, tetrahydrofuran (THF), succinic anhydride, anhydride pyridine, 4-dimethylaminopyridine (DMAP), N-hydroxysuccinimide (NHS), N,N'-dicyclohexylcarbodiimide (DCC) and triethylamine (TEA) were purchased from Sigma Aldrich (Milwaukee, WI). Dichloromethane (DCM), magnesium sulfate, dimethyl sulfoxide (DMSO), ethanol, acetone and sodium hydroxide (NaOH) were purchased from Thermo Fisher Scientific (Waltham, MA).

### 2.2.2. Synthesis of $\alpha$ -hydroxyl, $\omega$ -acrylate oligomeric lactic acid (HEALA-OH) <sup>8</sup>

A mixture of 2.69 g HEA and 5g lactide was placed in a 100ml round-bottom flask and melted under nitrogen at 58 °C. Stannous octoate (65  $\mu\text{l}$ ) was added and the mixture was heated at 110 °C under nitrogen for 1h, after which 1mg hydroquinone was added to the reaction mixture to inhibit free-radical polymerization of acrylate groups. The reaction mixture was dissolved in DCM, washed with 100 ml distilled water, and vacuum dried. The

product, HEALA-OH, with a moderate yield (43%) was confirmed by  $^1\text{H NMR}$ .

### **2.2.3. Synthesis of $\alpha$ -carboxylate, $\omega$ -acrylate oligomeric lactic acid (HEALA- COOH) <sup>8</sup>**

HEALA-OH (3.32g) was dissolved in anhydrous THF (30ml) in a 100 ml 3-neck flask at room temperature under nitrogen. Succinic anhydride (1g), anhydride pyridine (3 ml) and DMAP (0.122g) were subsequently added. The reaction mixture was stirred for 24 h at 50 °C under nitrogen. After cooling to room temperature, the solvent was evaporated under vacuum and the residue was dissolved in DCM followed by three washes with 0.1M HCl solution. The organic phase was dried over magnesium sulfate and concentrated in a rotary evaporator. The viscous liquid product, HEALA-COOH, was dried under vacuum at room temperature. The dry product with a yield of 81% was stored at 4 °C.

### **2.2.4. Synthesis of NHS Activated Lactic Acid Oligomers (HEALA-NHS) <sup>8</sup>**

HEALA-COOH (2.7 g) and NHS (0.72 g) were added in a flask containing anhydrous DCM (10 ml) under nitrogen. The reaction mixture was cooled to 0 °C, to which a solution of DCC (1.29 g) in 10 ml anhydrous DCM was added drop-wise. The reaction was stirred for 4 h at 0 °C, slowly warmed to room temperature and stirred for additional 24 h, followed by removing the insoluble by product by filtration. The filtrate was concentrated under reduced pressure and subsequently dissolved in anhydrous DCM before filtration. The final product, HEALA-NHS, with a yield of 58% was confirmed by  $^1\text{H NMR}$ .

### 2.2.5. Synthesis of HEALA-Modified HA HGPs (HEALA-HGPs) <sup>8,10</sup>

HA particles (10 mg) were dispersed in 5 ml H<sub>2</sub>O, to which 5.73  $\mu$ l of TEA was then added drop-wise. The mixture was stirred for 30 min at room temperature under nitrogen and 0.5g HEALA-NHS in 7 ml DMSO was added drop-wise. The reaction was carried out at 40 °C for 24 h. The modified particles were washed with DMSO, ethanol and acetone, and dried at 37 °C. The modified particles were dispersed in NaOH solution (0.1M in D<sub>2</sub>O) and were stirred at 37 °C overnight for further degradation. The hydrolytic products were analyzed by <sup>1</sup>H NMR.

### 2.2.6. Synthesis of CK2.1 Modified HA HGPs (CK2.1-HGPs) <sup>11-12</sup>

Hydrogel particles HGPs (5 mg) and the CK2.1 peptide (1 mg) were added into a vial containing 1ml of PBS at pH 7.4. The reaction was allowed to proceed overnight at room temperature, after which particles were washed with water, ethanol and acetone. Particles were collected by centrifugation at 2,000 rpm (20 min) in each washing step before vacuum drying. The supernatant obtained from the CK2.1 modified particle synthesis was analyzed to determine the amount of CK2.1 encapsulated within the particles. The conjugation efficiency was calculated using the following equation:

$$P1: \quad E_c = \frac{\frac{A_b - A_a}{A_b} \times W}{W_p} \times 100$$

where  $E_c$  was conjugation efficiency (%),  $A_b$  and  $A_a$  were the supernatant absorbance of peptide before conjugation and the supernatant absorbance of peptide after conjugation, respectively.  $W$  (mg) was the amount of peptide before conjugation and  $W_p$  (mg) was the

amount of peptide in synthesis. Using such method might lead to an over-estimate because the peptides calculated involved unconjugated peptides which were removed by subsequent wash steps.

### **2.2.7. In vitro Peptide Release**

CK2.1-HGPs (5 mg) were stirred at 37 °C in 5ml PBS. At determined time points, 0.2ml suspension were sampled and particles were separated from the supernatant by centrifugation at 2,000 rpm. The collected particles were dispersed in 0.2ml fresh PBS and subsequently added into the release solution. The supernatant absorbance was measured with the UV-Vis spectrometer at 280 nm<sup>13</sup>. The peptide concentration was determined using a standard curve constructed with a peptide concentration of 0.0095 to 0.30 mmol/l. Each experiment from 3 repeats was conducted.

## **2.3. Results and Discussion**

### **2.3.1. Synthesis of Degradable Linkers**

The general procedure for the synthesis of a heterodifunctional linker for the construction of CK2.1-HGPs is outlined in Figure 2.1. First, lactic acid was polymerized off the hydroxyl terminal group of HEA using a ring opening polymerization of lactide in the bulk phase with stannous octoate as a catalyst to form HEALA-OH. The number of degradable LA repeats can be used to control the release kinetics of the immobilized CK2.1 peptide. Obviously, incorporating more lactic acid units will lead to faster peptide release due to the

higher probability of ester cleavage. For coupling to HA, it was not possible to directly react the free hydroxyl group of HEALA-OH with HA because HA possesses carboxylic acid that would interfere with the reaction. To this end, the hydroxyl group of lactic acid was converted to a carboxylic acid through an esterification reaction with succinic anhydride to form HEALA-COOH. HEALA-COOH was subsequently converted to an activated ester (HEALA-NHS), which undergoes facile reaction with the residual hydrazide groups in HA HGPs<sup>14-15</sup>.

The successful synthesis of HEALA-OH was confirmed by <sup>1</sup>H NMR (Figure 2.2). The spectrum displayed characteristic resonances for the acrylate protons (a, b and c in Figure 2.2) at  $\delta$  6.4, 6.12 and 5.90 ppm and -CH (f in Figure 2.2) and -CH<sub>3</sub> (d in Figure 2.2) protons of lactic acid at  $\delta$  of 5.26 and 1.30 ppm, respectively. From the integration ratio of the -CH proton corresponding to the lactic acid units (d) to the -CH proton of the acrylate group (b), the number of lactic acid repeat units was estimated to be  $\sim 3$ .

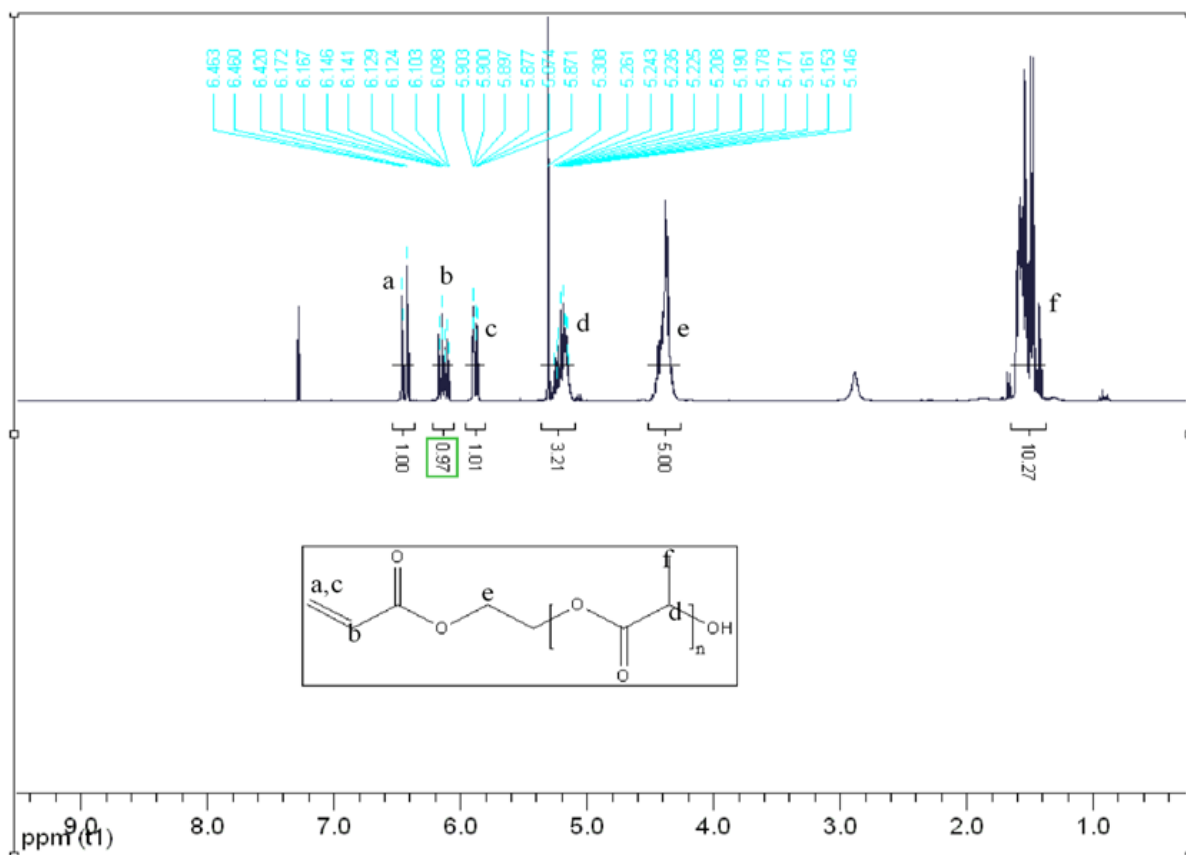


**Figure 2.2**  $^1\text{H}$  NMR spectrum of HEALA-OH. Solvent:  $\text{CDCl}_3$ .

The conversion of  $-\text{OH}$  to  $-\text{COOH}$  was also confirmed by  $^1\text{H}$  NMR (Figure 2.3). The  $\delta$  2.7 ppm resonance corresponding to the  $-(\text{CH}_2)_2$  protons (f, in Figure 2.3) of succinic anhydride were observed in the spectrum. The integration ratio of the  $-\text{CH}_2$  proton corresponding to succinic anhydride (f) to the  $-\text{CH}_2$  proton of HEA (e) was 1:1, confirming that carboxylate groups were introduced to the oligomers. The two unassigned peaks at 1.9 ppm and 3.9 ppm were attributed to THF remaining in the product.

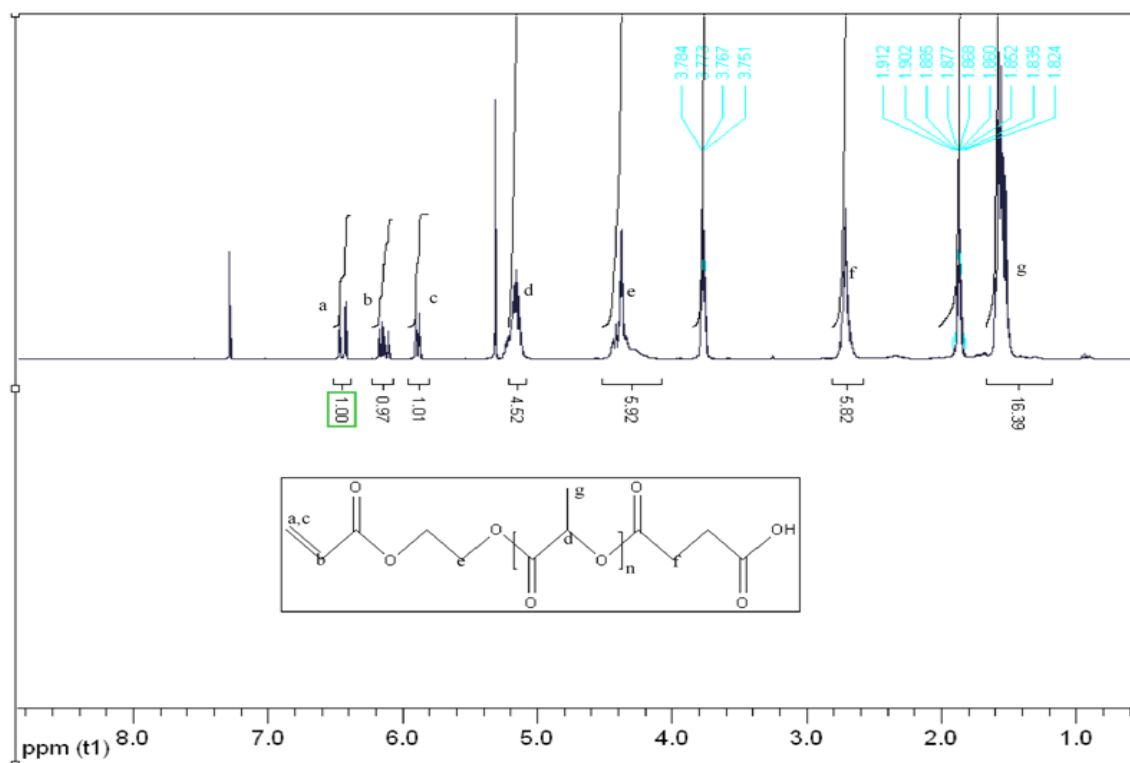


**Figure 2.3**  $^1\text{H}$  NMR spectrum of HEALA-COOH. Solvent:  $\text{CDCl}_3$ .

The NHS ester derivative was synthesized through the reaction of HEALA-COOH with NHS in the presence of DCC (Figure 2.1), where DCC promotes esterification by reacting with the end carboxyl group through nucleophilic substitution. The final product (HEALA-NHS) was confirmed by  $^1\text{H}$  NMR (Figure 2.4). The spectrum displayed peaks assigned to  $-\text{CH}_2$  protons corresponding to HEA (e), succinic anhydride (f) and the NHS functional group (g). The integration ratio of the  $-\text{CH}_2$  protons corresponding to HEA (e) to those corresponding to the succinic anhydride and the NHS functional group (g, f) was 1:2, confirming that the carboxyl group was converted to the NHS functional group.

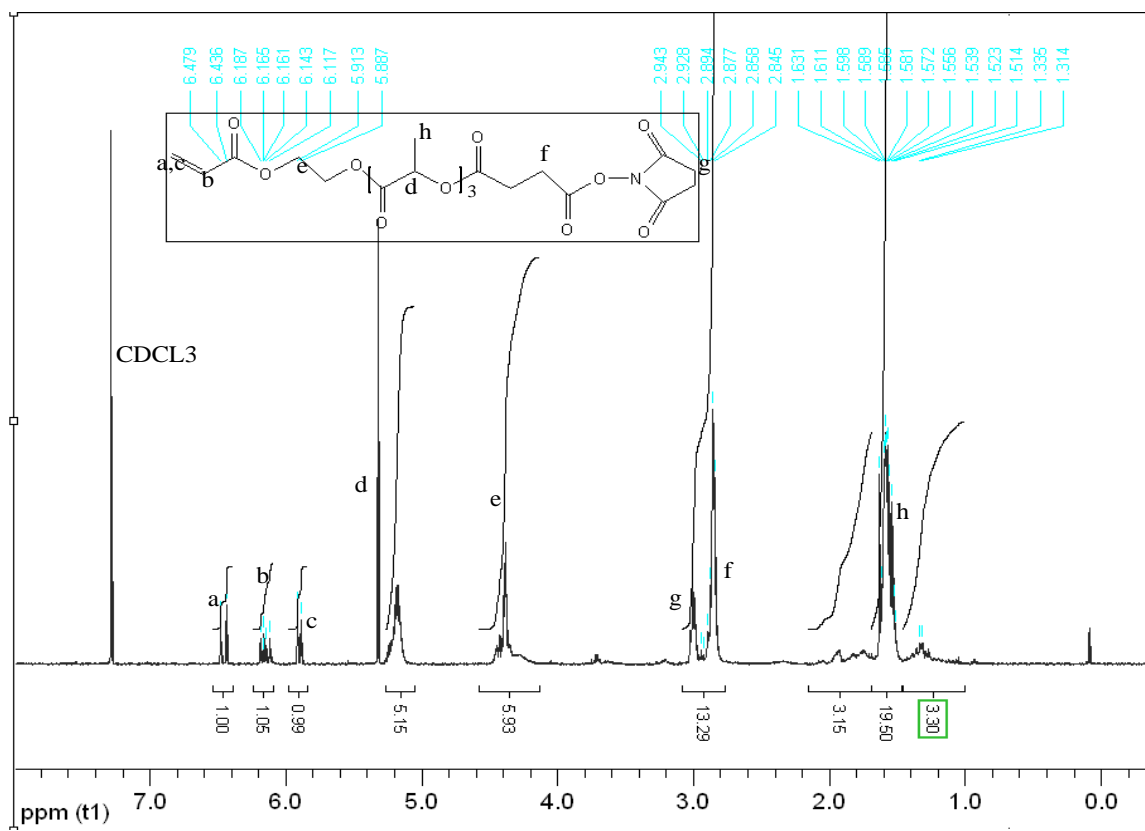


**Figure 2.4**  $^1\text{H}$  NMR spectrum of HEALA-NHS. Solvent:  $\text{CDCl}_3$ .

### 2.3.2. Synthesis of HEALA-HGPs

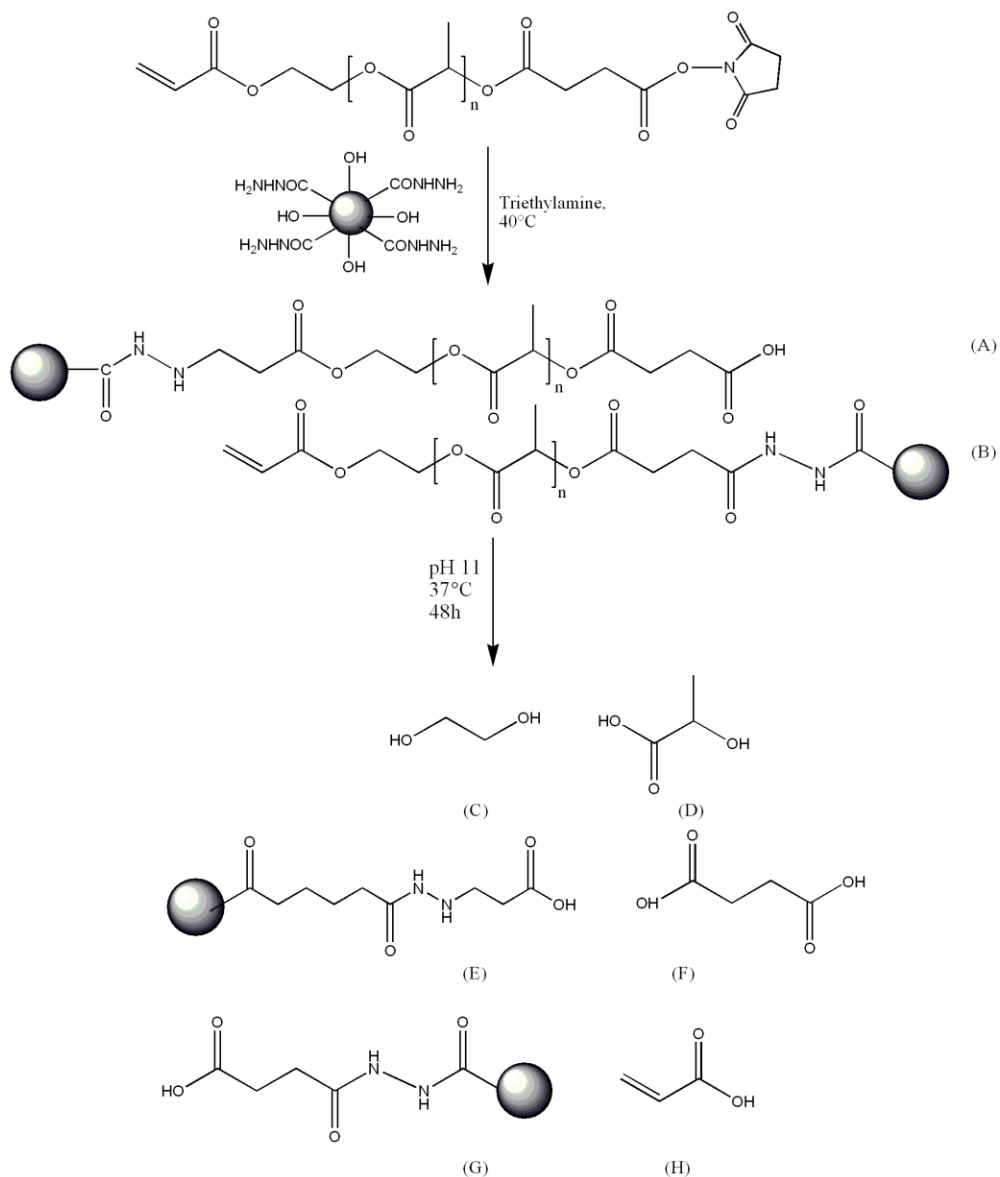


**Figure 2.5** Reaction scheme for the synthesis of HEALA-HGPs. The desired product, (A) formed via the nucleophilic substitution reaction between HGPs and HEALA-NHS. Michael addition reaction leads to a by-product, (B) that is not reactive towards cysteine-containing peptide. After degradation, products (A) were hydrolyzed into small molecules (C), (D), (E), (F) while products (B) were converted to be (C), (D), (G), and (H).

Previous research<sup>14, 15</sup> confirmed that during the particle synthesis, hydrazide groups from HAADH were not exhausted in the reaction with aldehyde groups from HAALD in the inverse emulsion process. Compared to hydroxyl groups (abundant in HA), hydrazides show enhanced reactivity at neutral and acidic buffer conditions<sup>16</sup>. Thus, the acrylate groups were introduced to the particles mainly via the nucleophilic reaction between NHS functional groups in HEALA-NHS and hydrazide groups in HA HGPs. Under the reaction condition employed, HEALA-NHS could also react with the hydrazide functionalities in HGPs via a Michael type addition reaction, consuming the acrylate groups by forming a stable C-N bond (B in Figure 2.6).

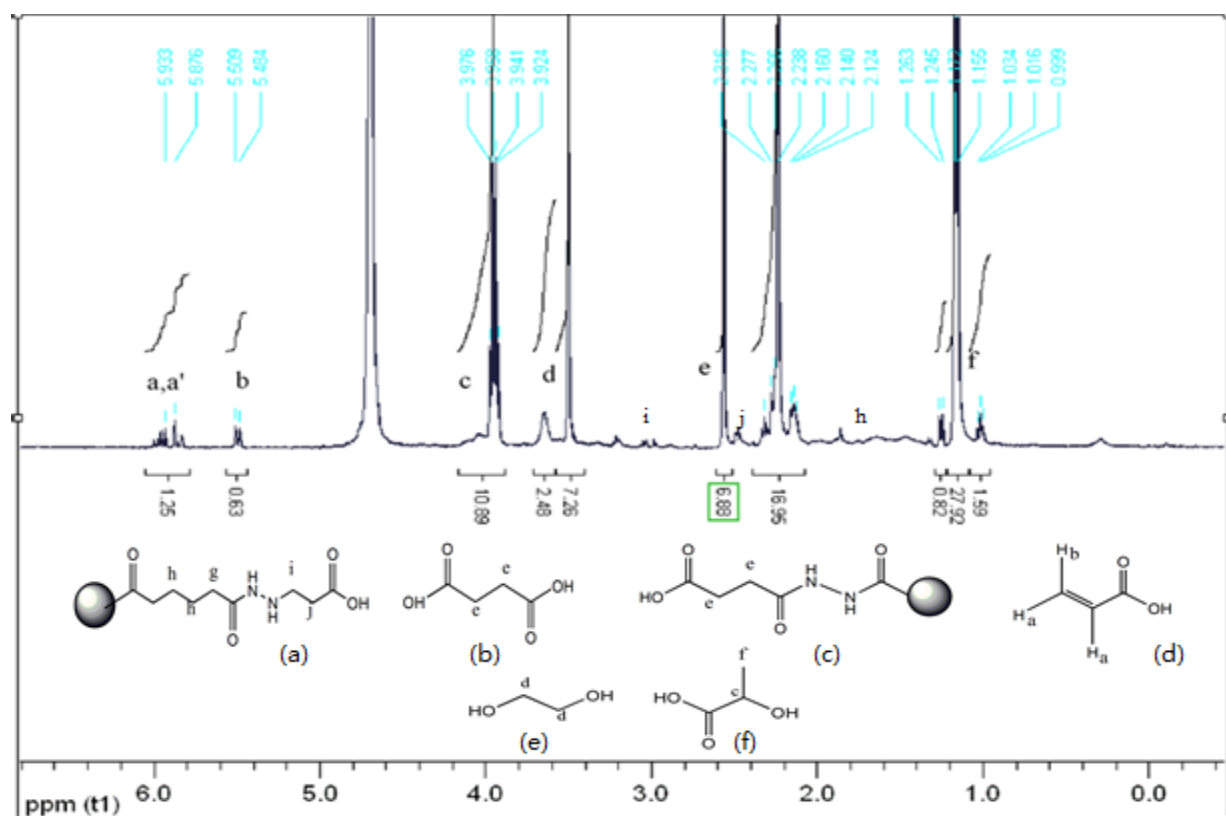


**Figure 2.6** <sup>1</sup>H NMR spectrum of acrylate modified particles after degradation. After degradation, by-products were hydrolyzed into small molecules (a), (b), (e), and (f) while main products were converted to be (c), (d), (e), (f).

The HEALA-HGPs were degraded into soluble molecules that were subjected to  $^1\text{H}$  NMR analysis. The spectrum (Figure 2.6) displayed characteristic resonances for the acrylate protons at  $\delta$  5.90 and 5.40 ppm, confirming the success introduction of acrylate groups to HA HGPs. According to the spectrum, peaks (i, j, h) resulted from the degradation of the by-product (B) were also present. However, these peaks are of low intensity, suggesting that the by-product B existed as a minor population. And peaks in the range of 3.6-4.0 ppm resulted from the degradation of HA were also present, which was overlapping with peaks c, d.

### 2.3.3. Peptide conjugation and release

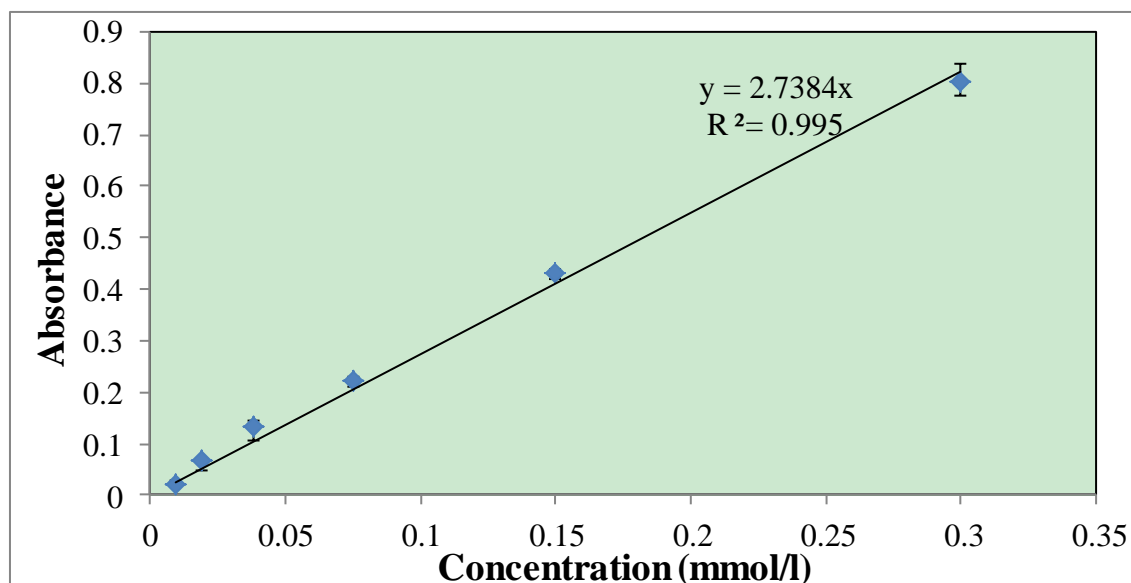


**Figure 2.7** Peptide standard curve obtained at 280nm

After the successful immobilization of hydrolytically cleavable acrylate groups to HA HGPs, the cysteine-containing CK2.1 peptide was conjugated to the particles via a Michael

reaction between the immobilized acrylates and cysteine thiol, forming a thiol-ether linkage. According to the equation P1, the conjugation efficiency of peptide was 10%.

Figure 2.8 shows the release of CK2.1 from HA HGPs at pH 7.4 for up to 7 days. The peptide concentration in the release media was quantified by monitoring the absorbance of the tryptophan (W) residue in the peptide using a standard curve (Figure 2.7). The formulation showed no burst release, and during 7 days peptide release continued until a plateau value was reached at 90% of the peptide loading. Each experiment from 3 repeats was conducted.

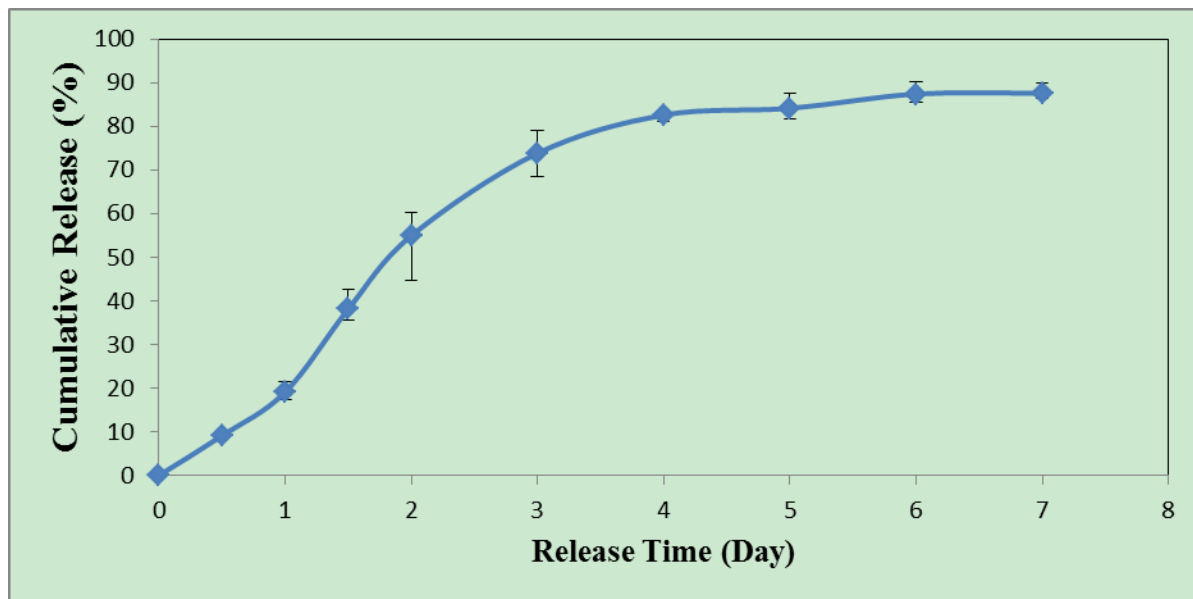


**Fig 2.8** Peptide release curve obtained at 280nm

## **2.4. Conclusion**

CK2.1 peptide was successfully conjugated to HA HGPs via a hydrolytically degradable linker. The peptide was released from HGPs in PBS at pH 7.4 in a controlled manner for up to 7 days.

## REFERENCES

- [1] Chester, N.; Marshak, D. R. *Analytical Biochemistry* **1993**, *209*, 284-290.
- [2] Coulais, Y; Marcelon, G; Cros, J.; Guiraud, R. *Pathologie Biologie (Paris)* **1983**, *31*, 577-582.
- [3] Marin, O.; Meggio, F.; Sarno, S.; Cesaro, L.; Pagano, M. A.; Pinna, L. A. *Biological Chemistry* **1999**, *274*, 29260–29265.
- [4] Nohe, A.; Keating, E.; Petersen, N.O. *Cell Science* **2003**, *116*, 3277–3284.
- [5] Uebelhart, D.; Williams, J. M. *Current Opinion in Rheumatology* **1999**, *11*, 427-35.
- [6] Cole, D. J.; Gattoni-Celli, S.; McClay, E. F; Metcalf, J. S.; Brown, J. M.; Nabavi, N.; Newton, D. A.; Woolhiser, C. B.; Wilson, M. C.; Vournakis, J. N. *Clinical Cancer Research* **1997**, *3*, 867-873.
- [7] Hahn, S. K.; Oh, E. J.; Miyamoto, H.; Shimobouji, T. *Pharmaceutics* **2006**, *322*, 44-51.
- [8] Sahoo, S.; Chung, C.; Khetan, S.; Burdick, J. A. *Biomacromolecules* **2008**, *9*, 1088–1092
- [9] Yun, Y. H.; Goetz, D.J.; Yellen, P.; Chen, W. *Biomaterials* **2004**, *25*, 147 – 157.
- [10] Al-Jammaz, I.; Al-Otaibi, B.; Okarvi, S.; Amartej, J. *Labeled Compounds and Radiopharmaceuticals* **2006**, *49*, 125–137.
- [11] Mather, B. D.; Viswanathan, K.; Miller, K. M.; Long, T. E. *Progress in Polymer Science* **2006**, *31*, 487–531.
- [12] Alderton, A. L.; Faustman, C.; Liebler, D. C.; Hill, D. W. *Biochemistry* **2003**, *42*, 4398–4405.
- [13] Ali, M. S.; Shenoy, B. C.; Eswaran, D.; Andersson, L. A.; Roche, T. E.; Patel M. S. *Biological Chemistry* **1995**, *270*, 4570 - 4574.
- [14] Jha, A. K.; Malik, M. S.; Farach-Carson, M. C.; Duncan, R. L.; Jia, X. Q. *Soft Matter* **2010**, *6*, 5045-5055.
- [15] Jha, A. K.; Yang, W. D.; Kirn-Safran, C. B.; Farach-Carson, M. C.; Jia, X. Q. *Biomaterials* **2009**, *30*, 6964–6975.

- [16] Raddatz, S.; Mueller-Ibeler, J.; Kluge, J.; Wäss, L.; Burdinski, G.; Havens, J. R.; Onofrey, T. J.; Wang, D.; Schweitzer, M. *Nucleic Acids Research* **2002**, *30*, 4793-4802.

## **Chapter 3**

# **CHONDROGENIC DIFFERENTIATION OF MESENCHYMAL STEM CELLS CULTURED IN HYALURONIC ACID-BASED DOUBLY CROSSLINKED NETWORKS**

### **3.1. Introduction**

Articular cartilage is a connective tissue populated by specialized cells of mesenchymal origin. The primary cells in cartilage are chondrocytes, which are responsible for producing, sustaining, and degrading ECM. Mature cartilage is vulnerable to injuries and disease processes that cause irreversible tissue damage because of a limited capacity for self-repair<sup>1</sup>.

Attempts to clinically augment cartilaginous healing responses have utilized two strategies, namely, stimulation of regeneration in situ or transplantation of replacement tissues. However, these methods generally produce fibrous tissue without desired mechanical and morphological characteristics<sup>2</sup>. Therefore, recently, the development of cell-based techniques that utilize a three-dimensional (3D) carrier mimicking the physiological microenvironment has changed the direction of research. These approaches, incorporating cells such as chondrocytes and perichondrocytes into a variety of carrier systems, including

HA and collagen gels<sup>3</sup>, have demonstrated an encouraging capacity for chondrogenic induction. Unfortunately, the slow *in vitro* propagation of adult chondrocytes has limited their widespread use<sup>4</sup>.

To overcome these shortages, MSCs have become a popular choice for cartilage engineering due to their capacity of rapid proliferation and differentiation. Researchers have shown that cell shape and curvature influence cell-fate decisions<sup>4,5</sup>. During morphogenesis, cells undergo dramatic changes in cell shape as they differentiate into different lineages. Osteogenic cells initially take on flattened morphology as they begin to calcify matrix, whereas chondrogenic and adipogenic cells round up in their early differentiation and myogenic cells extend into elongated spindles to execute their muscular functions<sup>6</sup>. The changes in cell shape can regulate the differentiation of mesenchymal progenitor cells. For example, fibronectin-induced cell flattening and spreading inhibits chondrogenic differentiation, which can be reversed by keeping cells in a round configuration or upon disruption of the cytoskeleton<sup>5</sup>. Chondrocytes taken from condensed articular cartilage and allowed to attach on a planar substrate down-regulate chondrocyte-specific markers. In particular, when grown in monolayer cultures, chondrocytes become flattened, lose their differentiated phenotype, and become dedifferentiated cells that synthesize molecules normally found in fibroblasts<sup>6</sup>. In this case, compared with 2D monolayers, 3D scaffolds are more suitable for introducing chondrogenesis. hMSCs are forced to round up and differentiate down the chondrogenic lineage more readily when cultured in a 3D microenvironment where cell-cell contact is

either present or mimicked<sup>6,7</sup>. In addition to the capability to help cells remain round in shape, 3D scaffolds offer a more reliable prediction of cell *in vivo* responses due to the existence of chemical and molecular gradients that precisely mimic *in vivo* ECM, contributing to intracellular signaling pathways, and provide a physiological environment for supporting and promoting key cell functions<sup>8-9</sup>. Thus, 3D, cell-degradable and cell-adhesive hydrogels could provide a unique platform in which to expand and differentiate hMSCs, allowing cells to spread, proliferate, and locally remodel their microenvironment in a manner that better mimics *in vivo* conditions.

In previous studies<sup>10-12</sup>, the utilities of HA for cartilage tissue repair were researched. The cartilage ECM is primarily comprised of collagen II, proteoglycans like aggrecan and glycosaminoglycans (sGAG). HA binds to aggrecan to form aggregates, providing compressive resistance to the tissue. The interactions between chondrocytes and HA help organize the ECM and stimulate chondrogenesis as well as the synthesis of more proteoglycans; therefore, HA was one of the most attractive scaffolding materials for directing cell chondrogenesis<sup>13-14</sup>.

Because MSCs encapsulated in HA-based hydrogels can be alive, this system is commonly used to study the cell activities involved in chondrogenesis. Our group has shown that when gelatin-conjugated HA particles were introduced to a photochemically crosslinked HA hydrogel matrix, MSCs were able to adhere to the matrix and proliferated readily.<sup>15</sup> However, in this study, cells were seeded on the surface of the hydrogels, displaying a

spread-out morphology and undergoing osteogenic differentiation. These results have provided a solid foundation for me to explore hydrogel properties that guide chondrogenic differentiation. In this study, MSCs were encapsulated in HA-based doubly crosslinked networks (DXNs) containing gelatin-conjugated HA hydrogel particles and were cultured in MSC growth media for up to 35 days. Our preliminary data suggest that MSCs in this type of matrix underwent chondrogenic differentiation. Cell proliferation, cell morphology and ECM production were quantified at various time points. The mechanical properties of the cell-free hydrogels and cell/gel constructs were analyzed by a commercial rheometer and a home-built torsional wave apparatus (TWA).

## **3.2. Materials and Methods**

### **3.2.1. Materials**

Hyaluronic acid (HA, sodium salt, 1.0 MDa and 500 kDa) was generously donated by Genzyme Corporation (Cambridge, MA). Light mineral oil, Span 80, 4-(dimethylamino) pyridine (DMAP), tetrabutylammonium bromide (TBAB), glycidyl methacrylate (GMA), 2,2-dimethoxy 2-phenylacetophenone (DMPA), and 1-vinyl-2-pyrrolidinone (NVP) were purchased from Aldrich (Milwaukee, WI). The initiator solution for photocrosslinking was prepared by dissolving DMPA in NVP with a concentration of 30%. Gelatin type B (from bovine skin), Alcian blue 8GX, Alizarin red S, Oil Red O, sodium cyanoborohydride ( $\text{NaBH}_3\text{CN}$ ), tetrabutyl-fluorescamine, sodium thiosulfate, and were purchased from Aldrich (Milwaukee, WI). Acetone, hexane, isoproponal, hydrochloric acid, sodium

hydroxide, ammonium hydroxide, sodium chloride, and ethanol were obtained from Thermo Fisher Scientific (Waltham, MA). Paraformaldehyde (16% in H<sub>2</sub>O) was obtained from Electron Microscopy Sciences (Hatfield, PA). Propidium iodide and Syto 13 were purchased from Genway Biotech, Inc (San Diego, CA). Tetramethyl rhodamine isothiocyanate (TRITC)-conjugated phalloidin was purchased from Millipore (Billerica, MA). Rabbit polyclonal anti-collagen type II antibody, Alexa Fluor 488-labeled secondary antibody (goat anti-rabbit IgG), Alamar Blue, and DAPI were obtained from Invitrogen (Carlsbad, CA). Mouse monoclonal anti-integrin  $\alpha_2\beta_1$  antibody and Alexa Fluor 488-labeled secondary antibody (goat anti-mouse IgG) were purchased from Santa Cruz Biotechnology (Santa Cruz, CA). Mouse polyclonal anti-collagen type I antibody was obtained from Abcam (Cambridge, MA). All antibodies were diluted in PBS containing 3% bovine serum albumin (BSA) and BSA was purchased from Jackson ImmunoResearch (West Grove, PA). Human mesenchymal stem cells, human mesenchymal stem cell growth media, and trypsin/EDTA solution were purchased from Lonza (Walkersville, MD).

### **3.2.2. Synthesis of Glycidyl Methacrylate-modified HA (HAGMA)**

HA was chemically modified with GMA following previously reported procedures<sup>16</sup>. Briefly, DMAP (6.4 molar excess relative to HA repeats), TBAB (2.7 molar excess) and GMA (20 molar excess) were added to an aqueous solution of HA (10mg/mL, 50 mL). The reaction was allowed to proceed under nitrogen in dark for 48 h. Upon addition of NaCl, HAGMA was precipitated in excessive amount of acetone, followed by collecting the product by centrifuge. The precipitation process was repeated twice. The final product was

re-dissolved in 300 mL H<sub>2</sub>O and dialyzed (MWCO 10,000) against 0.1 N NaCl for 24 h and DI H<sub>2</sub>O for another 24 h before freeze drying. The final product was analyzed by <sup>1</sup>H NMR.

### **3.2.3. Synthesis of Gelatin-Conjugated HA HGPs**

#### **3.2.3.1. Preparation of HA HGPs**

Prior to the preparation of HA HGPs, HA derivatives containing hydrazide (HAADH) and aldehyde groups (HAALD) were synthesized and characterized following established procedures<sup>17-18</sup>. Inverse emulsion polymerization was carried out by initially homogenizing 1mL HAADH solution (1wt% in de-ionized water) in light mineral oil (25 mL) containing 0.1 mL of Span 80 for 5 min using a Silverson L4R homogenizer (Silverson Machines Ltd., Cheshire, England) at 1500rpm. 1ml HAALD (1wt% in de-ionized water) was subsequently added drop-wise to the emulsion, which was then homogenized for another 5 min. The aqueous phase was evaporated overnight at 40 °C with constant stirring. Particles were subsequently washed with hexane, isopropanol, and acetone before drying overnight.

#### **3.2.3.2. Synthesis of Gelatin-conjugated HA-based Hydrogel Particles (HA gHGPs)**

HA HGPs (20 mg) were dispersed in a PBS solution (10 mL) containing 10 wt% gelatin at pH 7.4, and the mixture was stirred at 37 °C for 4 h, followed by adding NaBH<sub>3</sub>CN (5.8 mg) to the mixture. The reaction was allowed to proceed for an additional 4 h at 37 °C. After

exhaustive washing with water and vacuum drying, the modified particles were reacted with glycine (18mg) in DI H<sub>2</sub>O (5 mL) for 2 h at 37 °C. The final product was washed with water, isopropanol, and acetone before vacuum drying<sup>19</sup>.

### **3.2.3.3. Evaluation of Gelatin Conjugation**

Gelatin conjugation was qualitatively confirmed by fluorescamine staining in which acetaldehyde-treated HGPs (aHGPs) were used as negative controls<sup>15</sup>. aHGPs were produced by reacting HGPs (1 mg/mL) with acetaldehyde (10 mg) in the presence of NaBH<sub>3</sub>CN (0.8 mg/mL) in DI H<sub>2</sub>O at 37 °C for 2 h. Particles were collected by centrifugation at 3500rpm and subsequently washed with DI H<sub>2</sub>O, isopropanol, and acetone before vacuum drying. For fluorescent labeling, gHGPs or aHGPs were dispersed in 100 µL DI H<sub>2</sub>O, to which 2 µL fluorescamine acetone solution (5 mg/mL) was added. The mixture was stirred for 5 min, after which stained particles were collected by centrifugation (3500rpm) and imaged with a Zeiss 5 Live Duo Laser Scanning Microscope (LSM, Carl Zeiss Inc., Thornwood, NY).

### **3.2.3.4. Particle Size Analysis**

The average size and size distribution of HA HGPs and HA gHGPs were analyzed using a Coulter Counter Multisizer 3 (Beckman Coulter, Fullerton, CA). Prior to the measurement, HA HGPs were dispersed in isotonic solution (10 µg/mL).

### 3.2.4. MSC Culture in HA DXNs

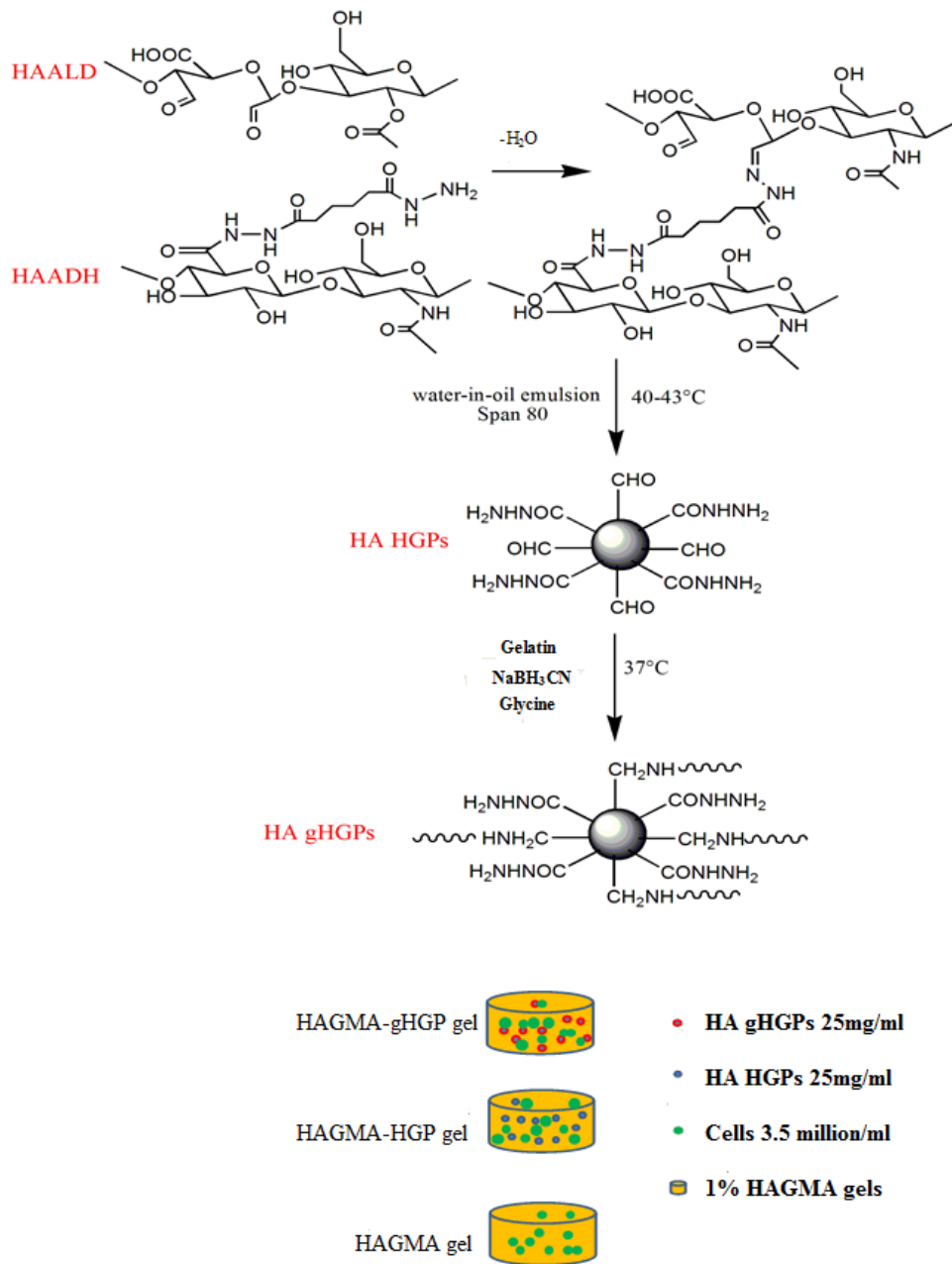


**Figure 3.1** Fabrication of three types of cell-seeded gels: the HAGMA-gHGP gel, the HAGMA-HGP gel and the HAGMA gel.

Human mesenchymal stem cells (passage 4) were seeded in a 150-cm<sup>2</sup> flask and cultured with 30 mL MSC growth media. After reaching confluence, cells were detached with 2 mL trypsin/EDTA solution at 37 °C for 10 minutes. The cells/media mixture was transferred into a centrifuge tube, where cells were counted with hemacytometer (Bright-line, 429918). Cells were collected after 5 min centrifugation at 1,000 rpm.

Hybrid constructs were prepared by entrapping gHGPs and cells in a photocrosslinked HAGMA matrix. Specifically, gHGPs were dispersed in HAGMA (1wt% in DI H<sub>2</sub>O) at a particle concentration of 2.5 wt%, and cells were subsequently mixed at a density of 3.5 million/ml. To this suspension was added 1.5 mL of the initiator solution. The mixture was thoroughly mixed and exposed to a long wavelength UV lamp (Model 100AP, Blak-Ray) for 10 minute to complete the gelation; the resultant gels were referred to as HAGMA-gHGP gels. Two types of control gels were also prepared. The first type of control gels (HAGMA-HGP gels) was prepared using HGPs in place of gHGPs, whereas the second type of control gels (referred as HAGMA gels) was prepared using HAGMA without particles. The cell-seeded hydrogels were cultured in MSC growth media at 37 °C in a humidified atmosphere with 5% CO<sub>2</sub>. Medium was refreshed every three days.

### **3.2.5. Cell Viability and Proliferation**

To assess cell viability, cell/gel constructs were rinsed with PBS and stained with propidium iodide (1/2000 dilution) and Syto 13 (1/1000 dilution) after 10, 20, and 30 days of MSC culture. Images were acquired using a Zeiss 5 Live Duo LSM with a Zeiss 40X

C-Apochromat (numerical aperture 1.2) water immersion objective lens. Cell proliferation was qualified with Alamar Blue. At a pre-determined time, the media were removed and replaced with fresh media containing 10% Alamar Blue. Fresh media containing Alamar Blue® were also added to hydrogels containing no cells, which were prepared using the same protocols above, as blank controls. All gels were then re-incubated at 37 °C, 5% CO<sub>2</sub> for 4 hours. A microplate reader (Victor<sup>3</sup> V Multilabel Counter, Perkin Elmer) was used to monitor the absorbance of Alamar Blue at 570 nm, using 600 nm as a reference wavelength to eliminate the instrument background. Each experiment was conducted in triplicates.

### **3.2.6. Cell Morphology and Focal Adhesion**

Cell adhesion and cell morphology were analyzed by immunofluorescence staining. Gel disks with different components were removed after 15 days of 3D culture, fixed in 4% paraformaldehyde for 1 h and washed twice with PBS. After permeabilization with PBS containing 0.1% Triton-X, cells were washed twice with PBS, blocked with PBS containing 3% BSA for 30 min at room temperature, and incubated with anti-integrin  $\alpha_2\beta_1$  mouse monoclonal primary antibody (1:100 with 3% BSA/PBS) overnight at 4 °C. Samples were washed three times with PBS, followed by incubation with Alexa Fluor 488 conjugated mouse secondary antibody (1:100 with 3% BSA/PBS) for 2 h and TRITC-conjugated phalloidin (1:100 dilution) for another hour at room temperature. Unbound secondary antibodies or phalloidin were removed by three washes with PBS. Finally, cell nuclei were stained with 1:1000 dilutions of DAPI for 10 minutes at room temperature before fluorescent visualization using a laser scanning confocal microscope (Zeiss 5 Live Duo

LSM).

### **3.2.7. Cell Differentiation**

Cells in all culture environments were removed after 30 days of culture. For immunofluorescence staining, gels were initially fixed in a 4% paraformaldehyde solution for 1 h, permeabilized with 0.1% Triton X-100 solution for 10 min, and treated with 3% bovine serum albumin solution. For histological staining, gels were embedded completely in OCT Compound (Tissue-Tek®), kept on dry ice, and subsequently cryosectioned at 25  $\mu\text{m}$ . Sections were stored at  $-20^{\circ}\text{C}$  for histological staining with Alamar Blue, Oil Red and Alizarin Red. In each washing step, excessive PBS was used to wash gels after treatment.

#### **3.2.7.1. Chondrogenesis**

Chondrogenic differentiation of MSCs was assessed through immunofluorescence staining of collagen II and aggrecan. Gels were divided into two groups, and each group included all three types of gels. Gels in one group were incubated with one type of primary antibody: rabbit polyclonal anti-collagen II antibody (1:100 with 3% BSA/PBS) or mouse monoclonal anti-aggrecan antibody (1:100 with 3% BSA/PBS), respectively, overnight at  $4^{\circ}\text{C}$ . Corresponding gels were subsequently mixed with 1:100 dilutions of the complementary secondary antibodies: Alexa Fluor 488 goat anti-rabbit antibody or Alexa Fluor 488 goat anti-mouse antibody for 2 h. Samples were treated with RITC-conjugated phalloidin (1:100 dilution) for another hour at room temperature and then incubated with DAPI (1:1000 dilution) for 10 min before fluorescent visualization. For each step,

excessive PBS was used to wash gels after treatment. Cell-seeded gels were treated with the same staining protocols except for incubation with the primary antibodies as the negative controls. Cell-free gels were prepared using the same protocols except for dispersing cells in HAGMA solution and were stained with the same methods as the blank controls.

Secretion of sGAG was assayed using Alcian blue histological staining. After being cryosectioned at 25 $\mu$ m, sections were fixed in 4% paraformaldehyde for 10 min and stained overnight with Alcian blue solution (0.5% in 3% acetic acid solution, pH 1) for 1h, followed by washing sections with room-temperature tap water until the water rinsed off clear. Staining results were recorded using a Nikon phase contrast optical microscope (Nikon, Kanagawa, Japan) with a Coolpix digital camera.

### **3.2.7.2. Osteogenesis and Adipogenesis**

Monitoring osteogenic differentiation of MSCs was accomplished through histological staining of calcium with Alizarin red and immunofluorescence staining of collagen I with antibodies. After cryosectioning, sections were fixed in 4% paraformaldehyde for 10 min and were stained with Alizarin red solution (2% in DI water, pH 4.2) in a 37 °C incubator for 20 min, and non-specific staining was removed by excessive washing with PBS until the removed PBS was clear. Cells were visualized via light microscopy and photographed. To test the secretion of collagen I in the matrix, gels were incubated with a 1:100 dilution of mouse monoclonal anti-collagen type I antibody overnight at 4 °C and goat anti-mouse

IgG-FITC (1:100 dilution) at room temperature for another hour.

Lipid deposition in adipogenesis was monitored by Oil Red staining. After cryosectioning, sections were fixed in 4% paraformaldehyde for 10 min and incubated with Oil Red O solution (0.3% in isopropanol) for 10 min at 37 °C, followed by washing sections with excessive isopropanol until the isopropanol rinsed off clear. Cells were visualized via light microscopy and photographed.

### **3.2.8 Hydrogel Mechanical Properties**

#### **3.2.8.1. Traditional Rheological Characterization**

For the rheology measurements using the commercial rheometer (AR2000, TA Instrument, New Castle, DE), gels were prepared using the protocols introduced in Chapter 3.2.4 and placed on the rheometer plate. Gels was subjected to a very slight pre-compression, in order to ensure its upper and lower surfaces to be parallel with the rheometer plates. And mineral oil was applied around the geometry to prevent samples from drying out during the measurement with a controlled strain of 0.1%. All measurements were carried out at 37 °C using a Peltier plate and performed within the linear viscoelastic region: the applied strain was 0.1%. During the test, frequency was swept from 0.1 Hz to 10 Hz and the storage ( $G'$ ) and loss ( $G''$ ) modulus were measured with three repeats.

#### **3.2.8.2. TWA Characterization**

In torsional wave experiments<sup>20-21</sup>, samples were sandwiched between two vertically

aligned acrylic plates. During the test, frequency was swept from 10 to 100 Hz while amplification factors were recorded. The representative frequency-dependent amplification factors for the best-fit model along with the experimental data were measured based on the average values from three consecutive measurements on one gel. Each experiment on one type of gels was conducted from three repeats. The shift of resonance frequencies was influenced by the width and height of different samples.

### **3.2.9. Statistical Analysis**

Means  $\pm$  standard error of means (S.E.M.) were calculated with three repeats, and statistically significant differences between two groups were determined using the Student t-test at  $P < 0.05$  (Excel, Microsoft).

## **3.3. Results and Discussion**

### **3.3.1. Synthesis of HAGMA.**

Soluble HAGMA was successfully synthesized following an established procedure<sup>16</sup>. A methacrylation degree of ~10% was determined by comparing the relative integrations of the vinyl protons (b and c at 5.6 and 6.1 ppm in Figure 3.2) and methyl protons in HA (a at 1.8 ppm in Figure 3.2) from the <sup>1</sup>H NMR spectrum of HAGMA (Figure 3.2).

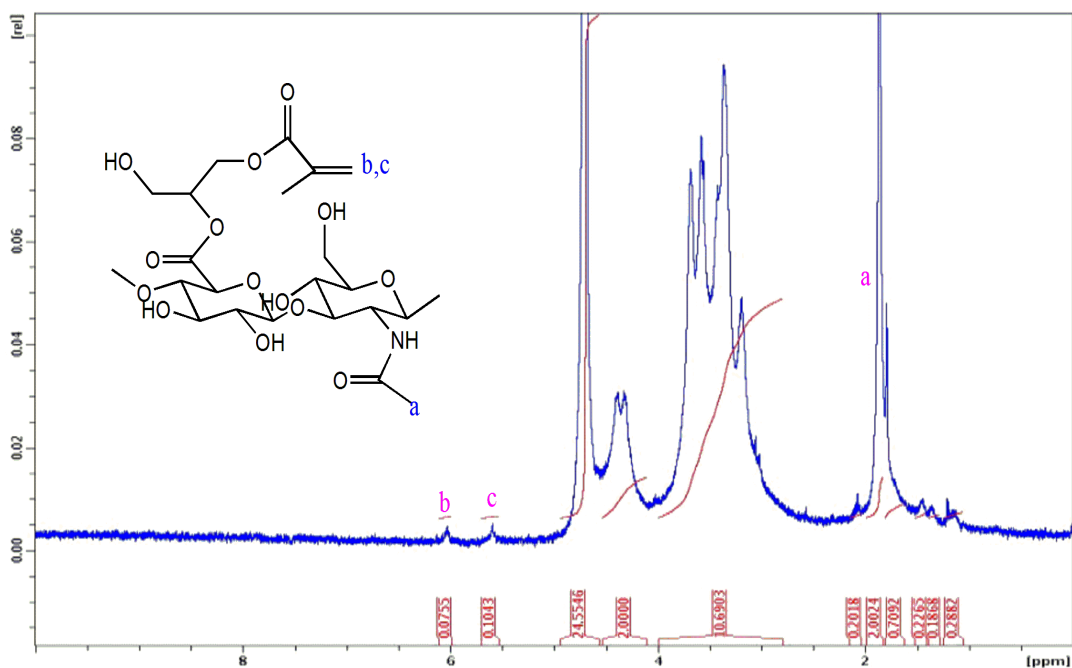


**Figure 3.2**  $^1\text{H}$  NMR spectrum of HAGMA. Solvent:  $\text{D}_2\text{O}$ .

### 3.3.2. Synthesis and Characterization of HA gHGs

Gelatin conjugation was qualitatively confirmed by fluorescamine staining<sup>15</sup>. Acetaldehyde blocked the hydrazide group of HA HGPs, and gelatin-conjugated particles were stained blue by fluorescamine due to its reaction with lysine amines in gelatin (Figure 3.3(A))<sup>15</sup>. Thus, the fluorescamine staining confirmed the success gelatin-conjugation.

The average size and the size distribution of HGPs and gHGs were analyzed by a Coulter counter (Figure 3.3(B)). The two types of particles had similar size distributions, thus, gelatin conjugation did not change particle size nor did it induce particle aggregation.

### 3.3.3. Cell Viability and Proliferation

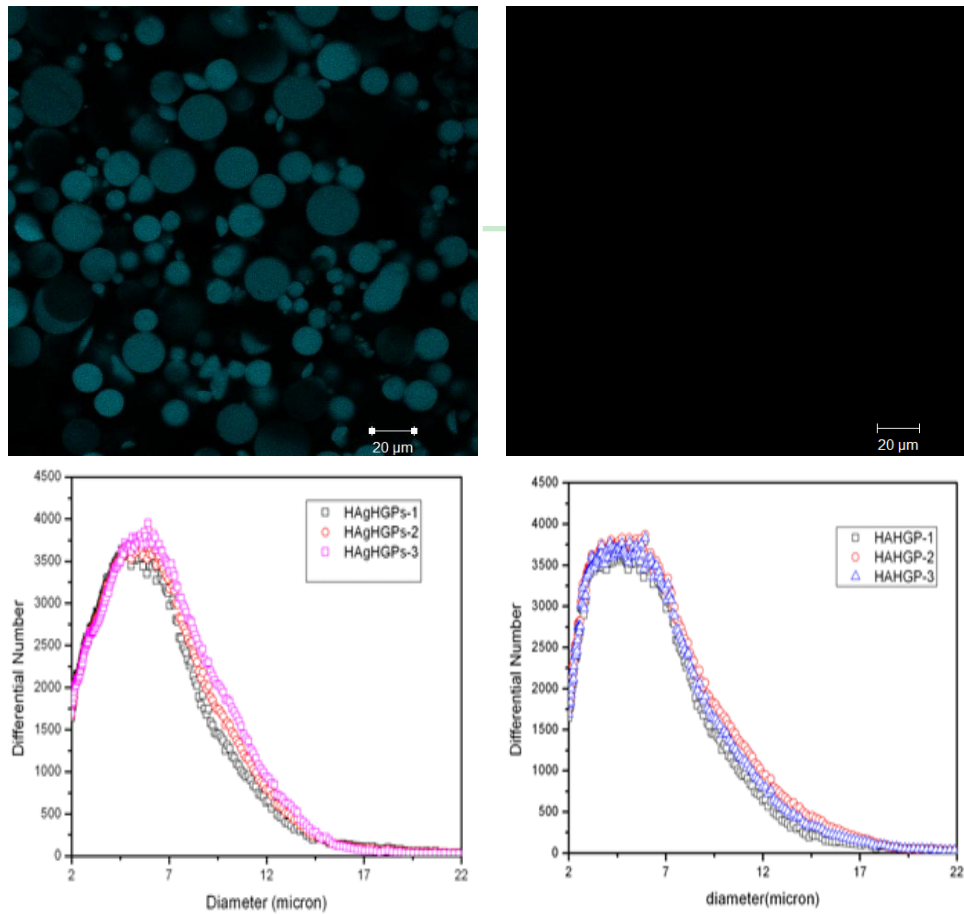
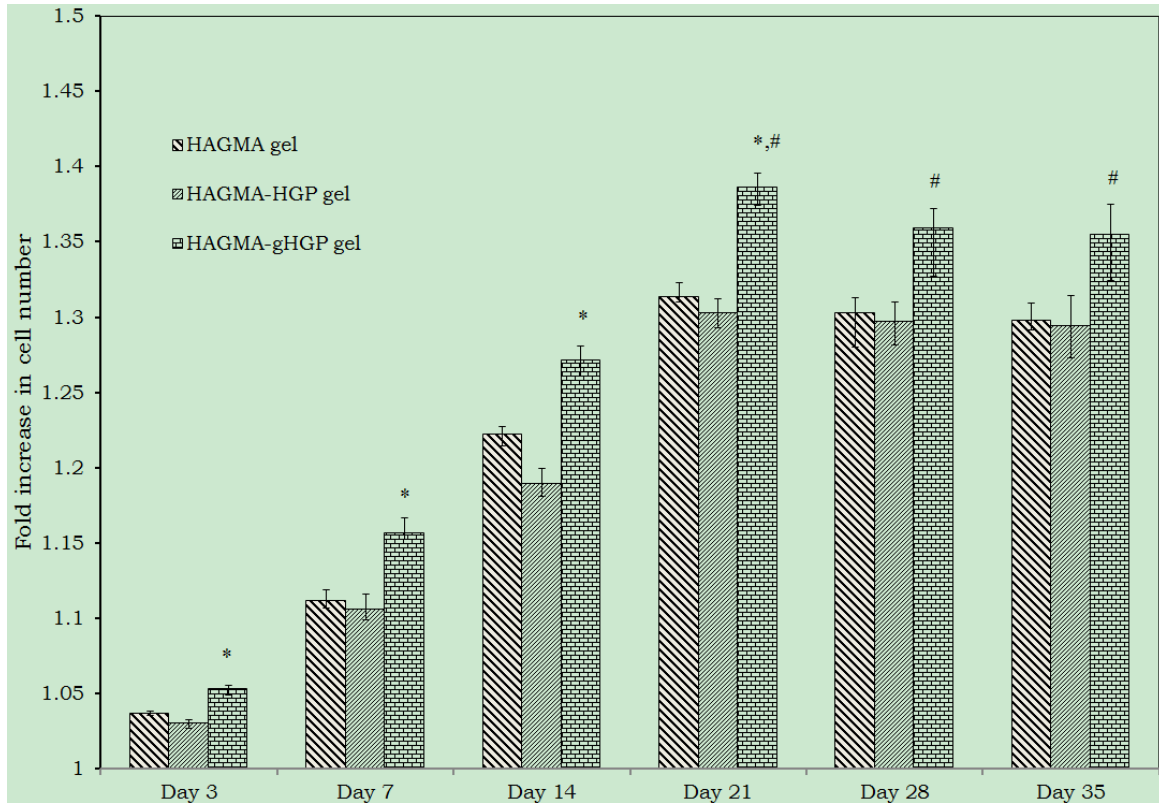


**Figure 3.3** (A) Fluorescamine staining of gelatin conjugated HA HGPs (left) and unmodified HA HGPs (right); (B) Particle size distribution measured by coulter counter; Mean size: 6-7 μm. Three repeating samples were used for each type of particles.

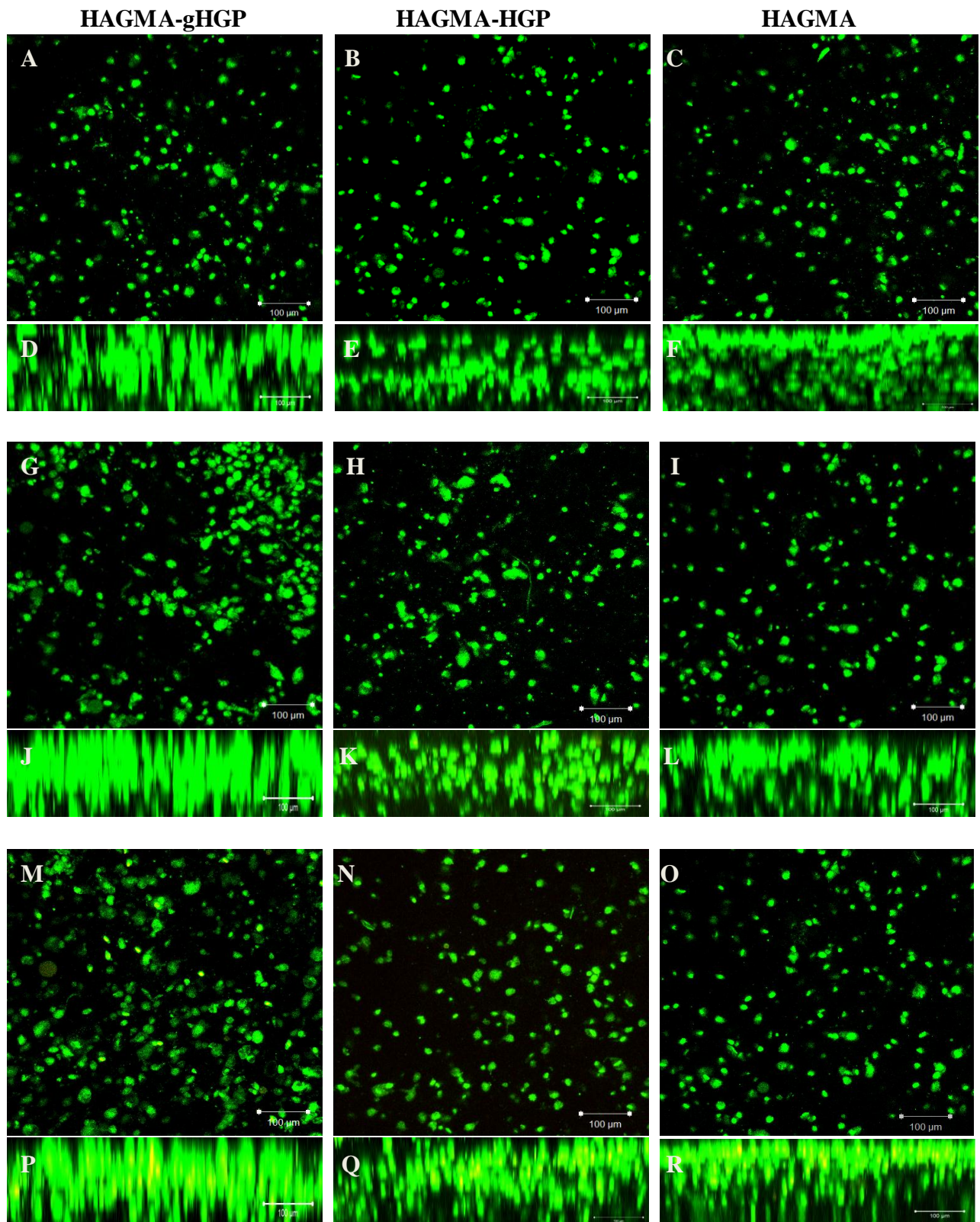
It is clear that HAGMA gels are composed of homogeneously distributed pores of submicron size range<sup>11</sup>. As demonstrated by Jha et al., both HAGMA-HGP gels and HAGMA-gHGP gels contain densely nanoporous particles surrounded by a loosely interconnected secondary matrix that exhibits morphology similar to the HAGMA matrix. When particles were physically entrapped in the HAGMA matrix, a depletion zone around

the hydrogel particles was created, even though particles and the secondary network were synthesized from the same starting materials.

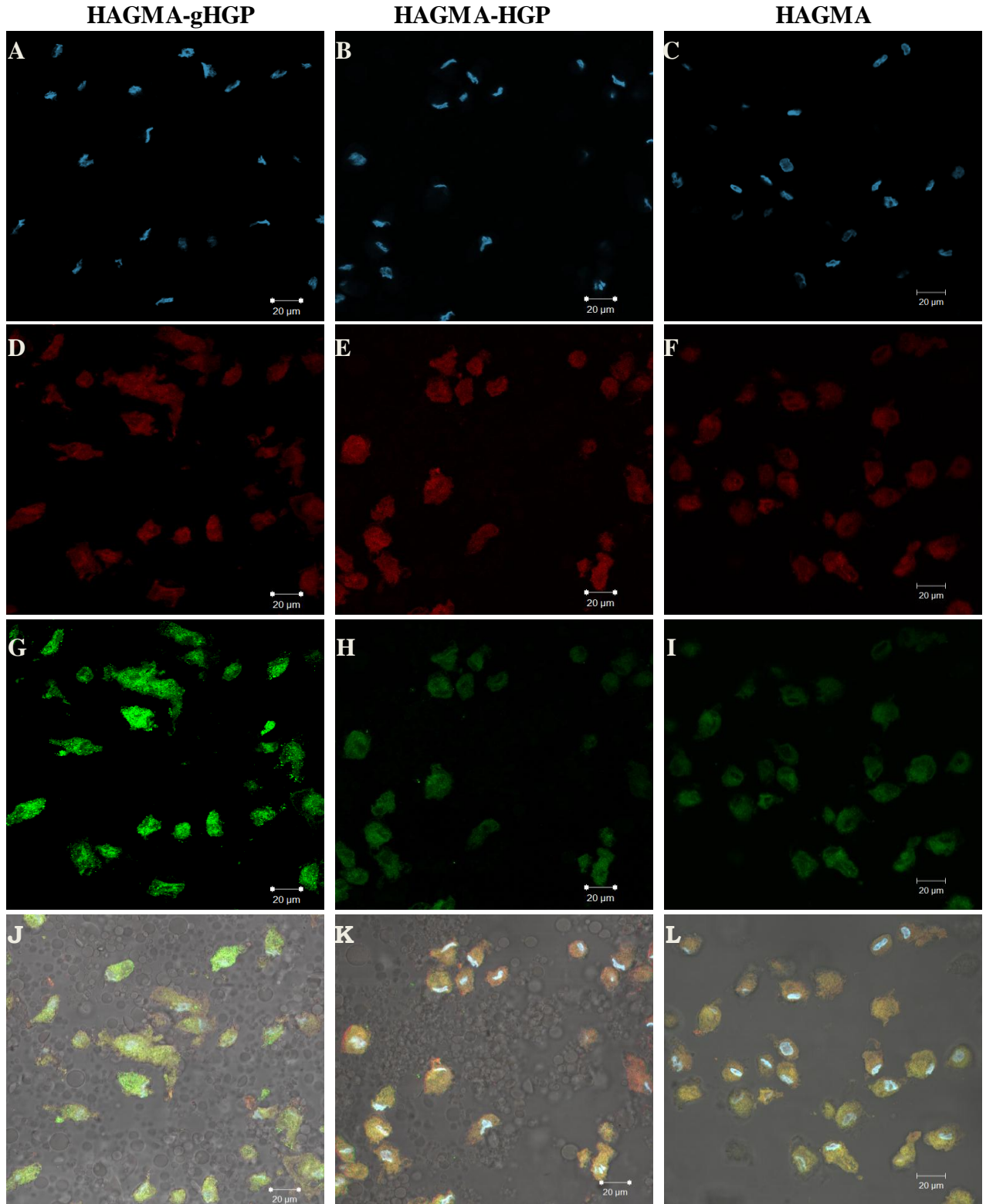
Alamar Blue assay was used to quantify cell proliferation in HA gels. The cell number in HAGMA-gHGP gels at day 7, 14, 21 was significantly different from that in HAGMA-gHGP gels at the previous time point. At day 21, 28 and 35, the cell number in HAGMA-gHGP gels was significantly different from that in HAGMA gels. Cells in HAGMA-gHGP gels proliferated more readily than those in other types of gels during the first 21 days, possibly due to gelatin's involvement in directing cell adhesion and proliferation<sup>22-23</sup>. A 1.4 fold increase in cell number at day 21 relative to that at day 0 was observed when MSCs were cultured in HAGMA-gHGP gels. After 21 days of MSC culture, the number of cells in HAGMA, HAGMA-HGP and HAGMA-gHGP gels is not significantly different from that at the previous time point. Live/dead staining revealed that cells were homogeneously distributed in both HAGMA-gHGP gels and HAGMA-HGP gels (Figure3.5). At these time points, cells were alive throughout the gels.



**Figure 3.4** Cell proliferation measured by the Alamar Blue assay during 35 days of culture in gels (normalized to the original cell-seeding number). \* indicates cell number was statistically significantly different from that at the previous time point,  $p < 0.05$ . # indicates cell number was statistically significantly different from that in HAGMA gels at the same day,  $p < 0.05$ .



**Figure 3.5** Live/dead staining of cells (A-F) after 10 days, (G-L) after 20 days and (M-R) after 30 days of hMSC culture in gels. (A-C, G-I, M-O): Top view projection of all z-series sections. (D-F, J-L, P-R): Side view projection of all z-series sections. Live cells were stained green while dead cells were stained red.



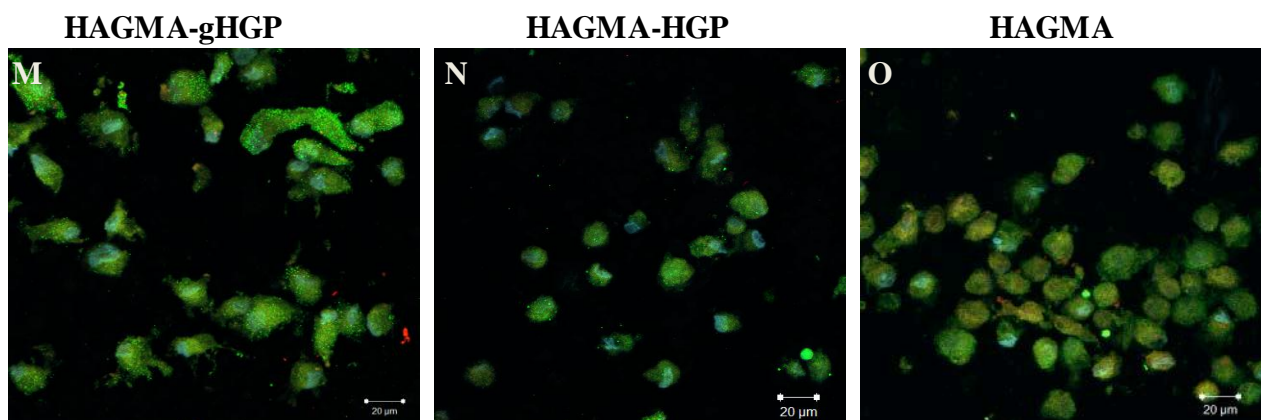


**Figure 3.6** Immunostaining of MSCs after 15 days of culture in HA gels. (A-L) One slide view for gels: (A-C) nuclei staining with DAPI (blue); (D-F) F-actin staining with rhodamine phalloidin (red); (G-I) integrin staining with primary anti-integrin  $\alpha_2\beta_1$  antibody and Alexa Fluor 488 goat anti-mouse antibody (green) (J-L) Overlay of staining in three channels and particles in phase contrast mode. (M-O) Top view projection of all z-series sections for gels

### 3.3.4. Cell Morphology and Focal Adhesion

The immunostaining of F-actin, integrin, and nuclei (Figure 3.6) showed that in all three types of gels, cell remained round after 15 days of culture. In 3D scaffolds, cells were forced into a rounded morphology and had limited spreading capabilities, leaving those adhesion-dependent cells to undergo possible chondrogenesis<sup>24</sup>. In cell-adhesive scaffolds, HAGMA-gHGP gels, cells did not significantly elongate but rather probed their environment by extending short, randomly oriented morphology with an increase in cell area<sup>25</sup>. Additionally, the integrin-based focal adhesion clusters were stained (Figure 3.6 (G-M)) in bright green areas in HAGMA-gHGP gels.

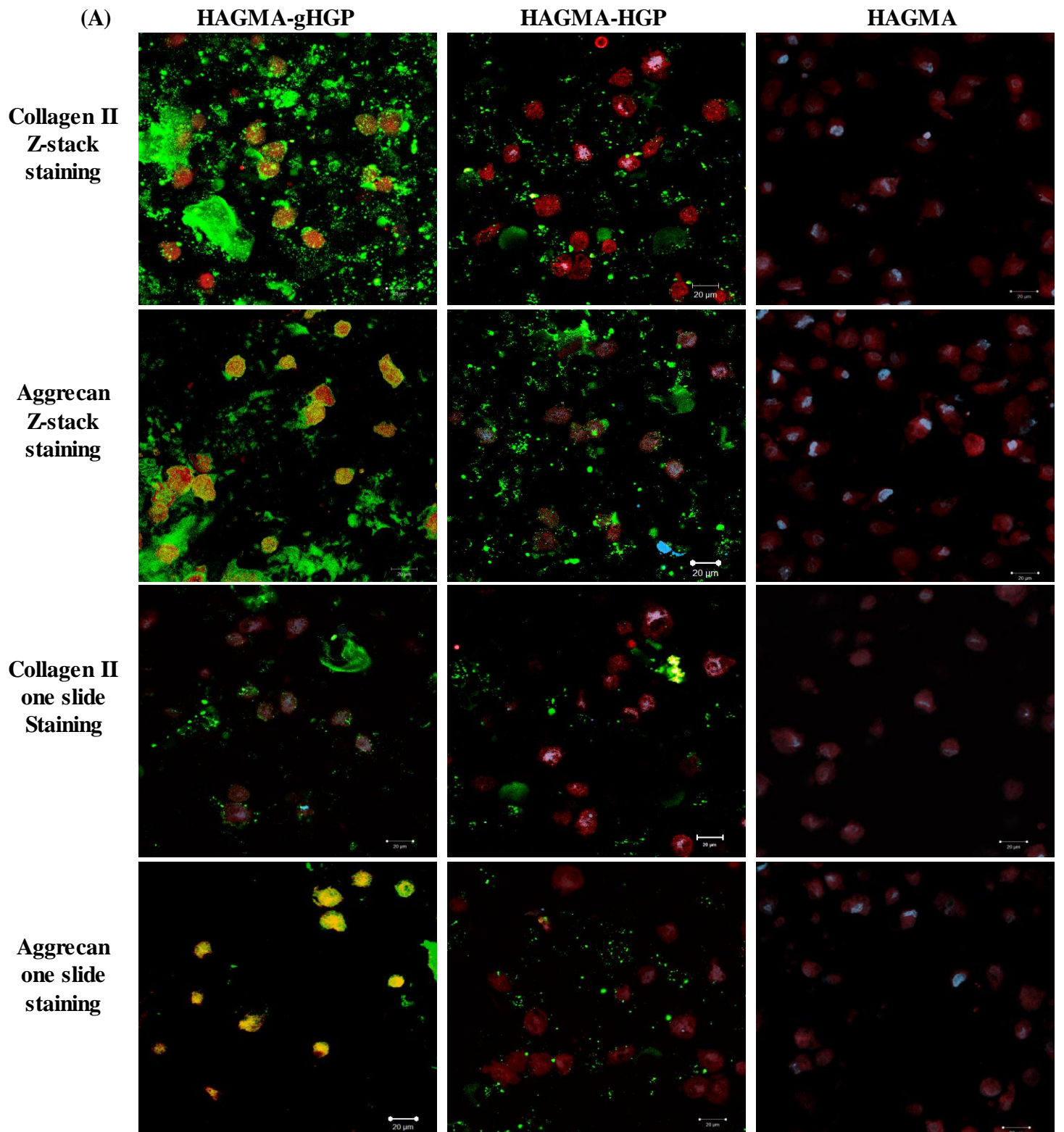
Ahrens et al proved that the initiation of chondrogenesis is cell shape-dependent. The round shapes indispensably provided conditions for chondrogenesis<sup>26-27</sup>. The

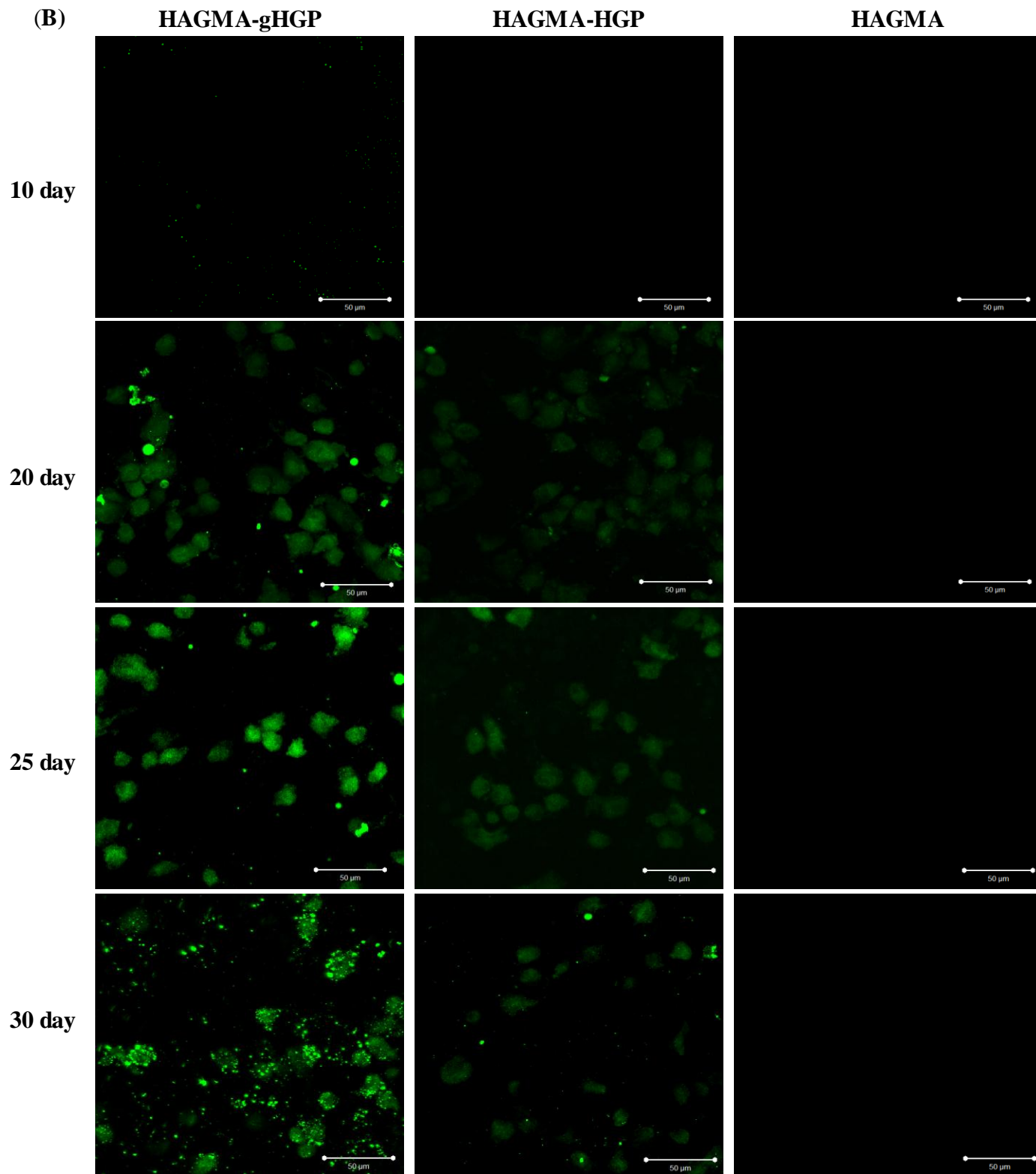
cells showed round shapes in HAGMA-gHGP gels, which provided prerequisites for chondrogenesis.

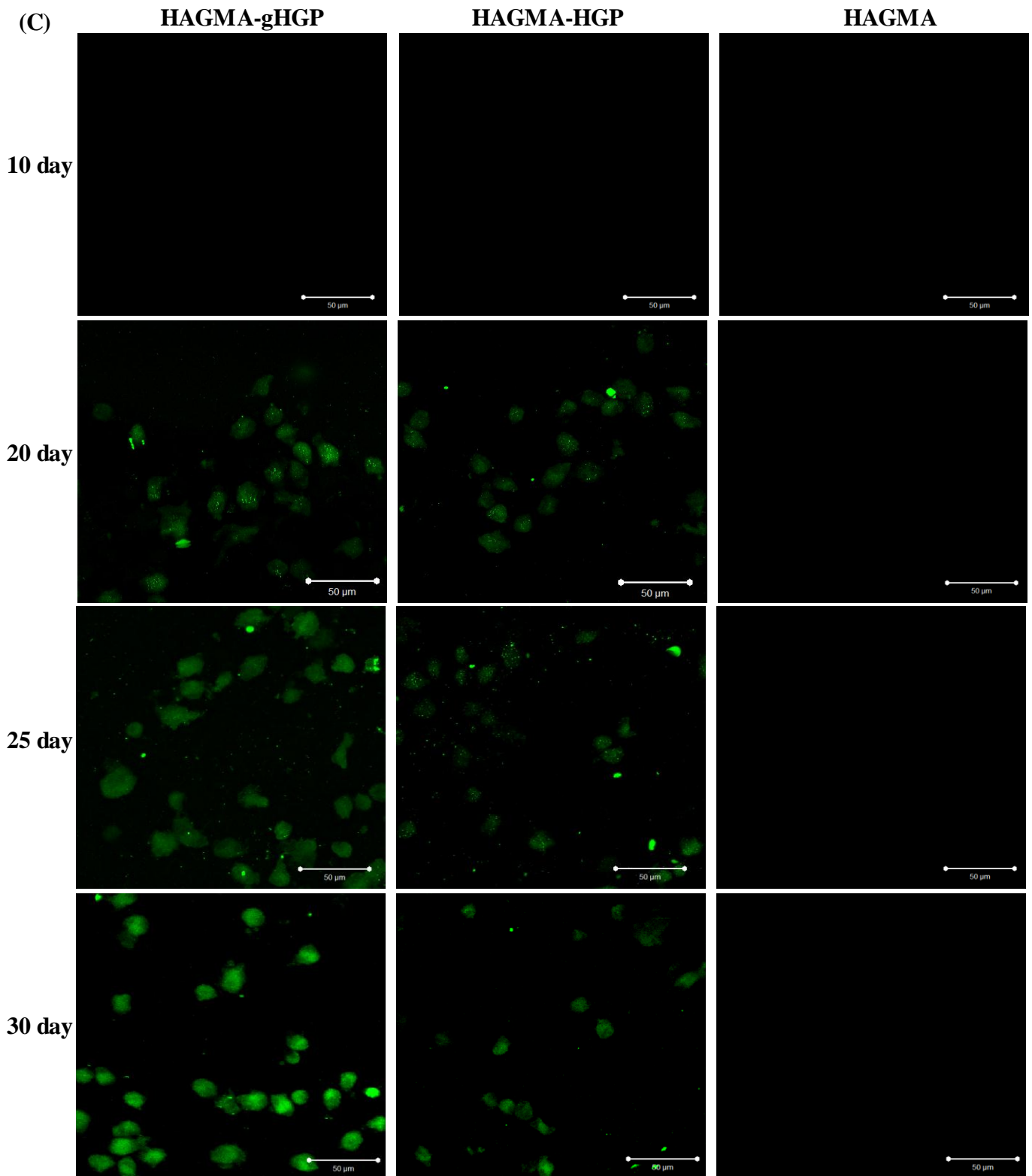
### **3.3.5. Cell Differentiation**

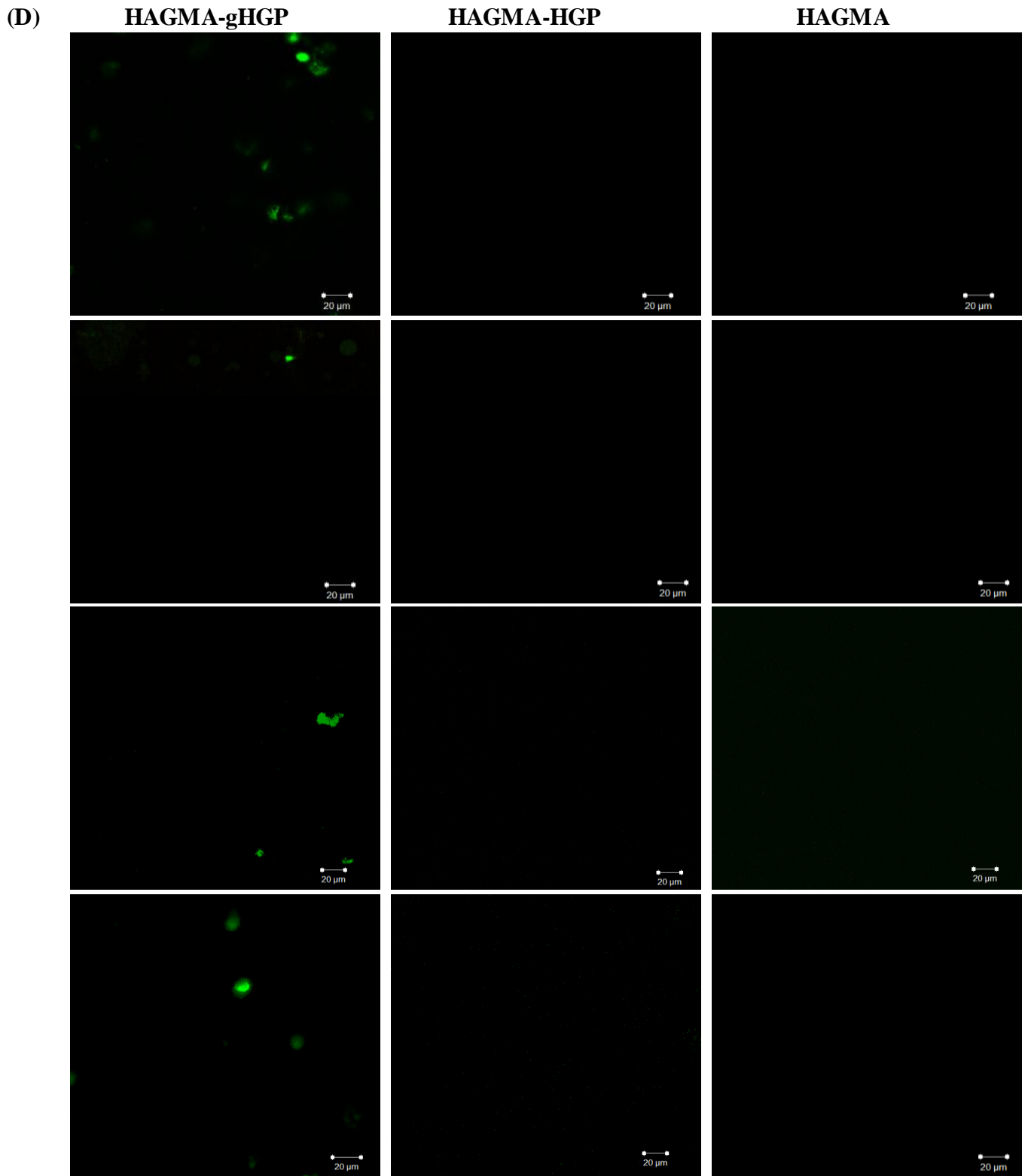
Figure 3.7 shows the immunostaining of cartilage specific ECM proteins (collagen II and aggrecan). Our results showed an increased accumulation of collagen II and aggrecan around the cells in HAGMA-gHGP gels. In HAGMA-HGP gels, only a small amount of collagen II and aggrecan was secreted around the cells. In HAGMA gels, cells did not synthesize any collagen II and aggrecan after 30 days of culture. The collagen II/aggrecan negative control groups proved that there was no non-specific binding between the HA-based hydrogels and antibodies used in experiments while there was a trace amount of non-specific bindings between gelatin-modified hydrogels and antibodies <sup>28-30</sup>.

In addition to the round shape of cells and cell-cell interaction, focal attachment was also important for cell differentiation. In HAGMA-gHGP gels, cell differentiation was enhanced by gelatin-modified scaffolds, evidenced by a significant increase in matrix secretion.









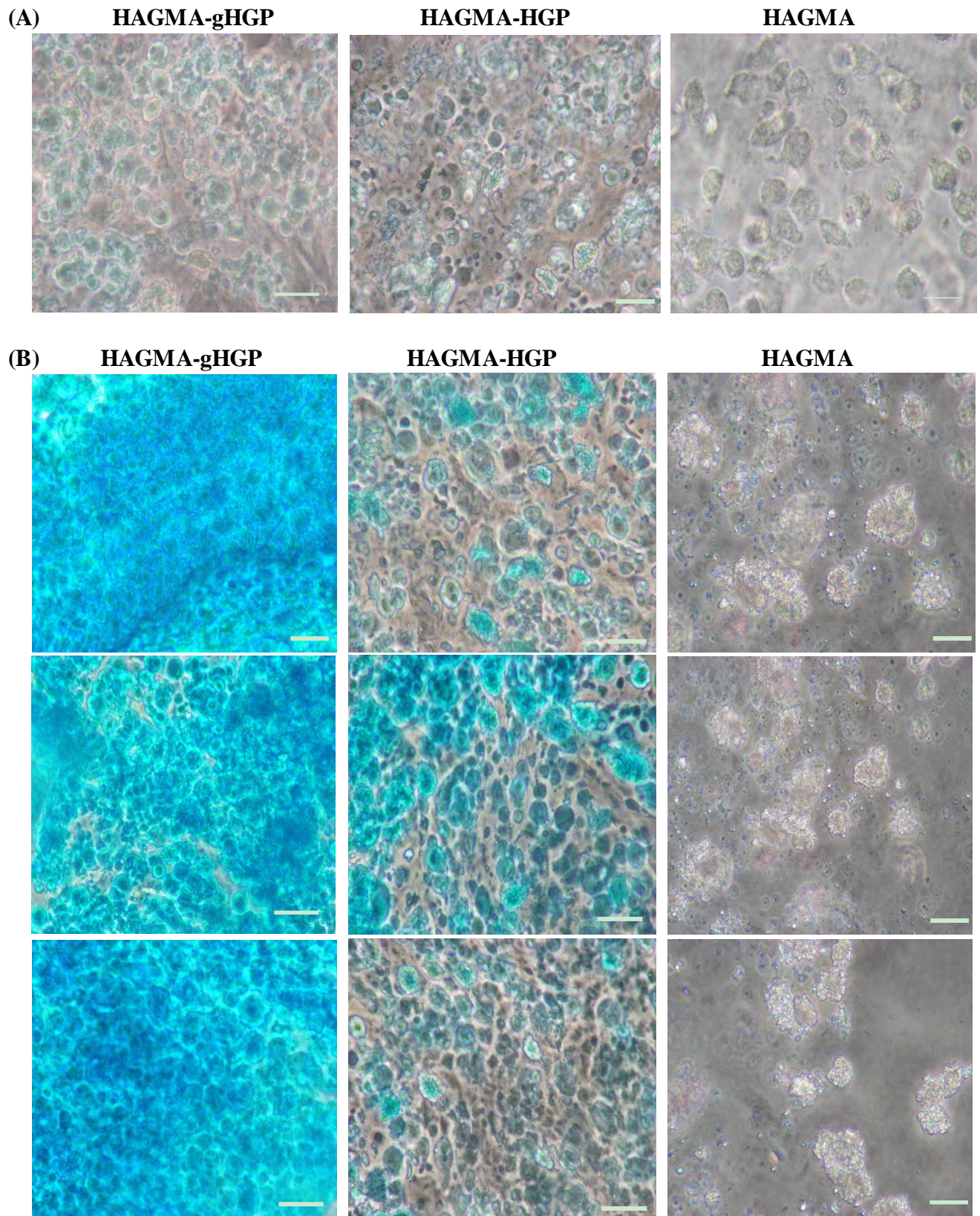
**Figure 3.7** Immunostaining of (A) collagen II and aggrecan (Z-stack projection and one slide comparison), (B) collagen II, (C) aggrecan and (D) blank controls and negative controls for collagen II and aggrecan staining. (A): All cells had stained F-actin and nuclei as reference. (B), (C): projection of a Z-stack reconstruction image of cells after 10, 20, 25 and 30 days of MSC culture in three types of gels.

Figure 3.7 (B, C) showed that cells produced increasing collagen II and aggrecan into the HAGMA-gHGP gels over time after 20 days of MSC culture. Cells also produced collagen II and aggrecan into the HAGMA-HGP gels, but more intense staining was clearly visible in HAGMA-gHGP gels. Cells did not produce collagen II and aggrecan in HAGMA gels.

Additionally, Alcian blue staining (Figure 3.8) showed sGAG deposition in the extracellular regions at day 30, indicating the sGAG was able to diffuse throughout the HAGMA-gHGP gel. Alcian blue staining showed that no sGAG was stained when MSCs initially were entrapped in all three types of gels, which showed that there was non-specific or specific binding between HA-based hydrogels and Alcian blue at pH 1, and Alcian blue could be completely removed from hydrogels by excessive washing in this case. After 30 days of culture, sGAG synthesis occurred in HAGMA-gHGP and HAGMA-HGP hydrogels, but a significantly higher amount of sGAG was detected in the three random areas in the former gels. Cells did not produce sGAG in HAGMA gels. Collagen II, aggrecan, and sGAG were major constituents of articular cartilage. In our experiments, secretion of those matrix depositions was also important in the process of chondrogenesis. In this experiment, three types of gels, which were prepared by 1% HAGMA macromere solution, probably had local degradation after 30 days of culture. Cells secreted some matrix deposition to fill the pore spaces. Due to local degradation of HAGMA-gHGP gels, the pore space should increase, which might lead to cell spreading and thus might inhibit the initiation of chondrogenesis. However, cells could avoid such change and retain a round shape as they become nested within the lacunae formed by their secretion of cartilage ECM molecules including aggrecan,

collagen type II, and sGAG<sup>31</sup>.

MSCs are fibroblastoid multipotent adult stem cells with a high capacity for osteogenic and adipogenic differentiation<sup>32-33</sup>. Calcium and collagen I were synthesized by osteoblast while lipids were the main matrix depositions secreted by adipocyte. Staining results with Alizarin red, Oil Red, and collagen I-related antibodies (Figure 3.9) showed negligible amounts of Alizarin red staining (calcium deposition), Oil Red staining (lipid deposition), and collagen I antibody staining in all three types of gels, indicated that cells were not differentiated into osteocytes or adipocytes after 30 days of culture.



**Figure 3.8** Histological staining of GAGs with Alcian Blue for (A) MSCs (B) differentiated cells after 30 days of culture in three random areas of gels after cryostat sectioning. Scare bar: 50  $\mu$ m

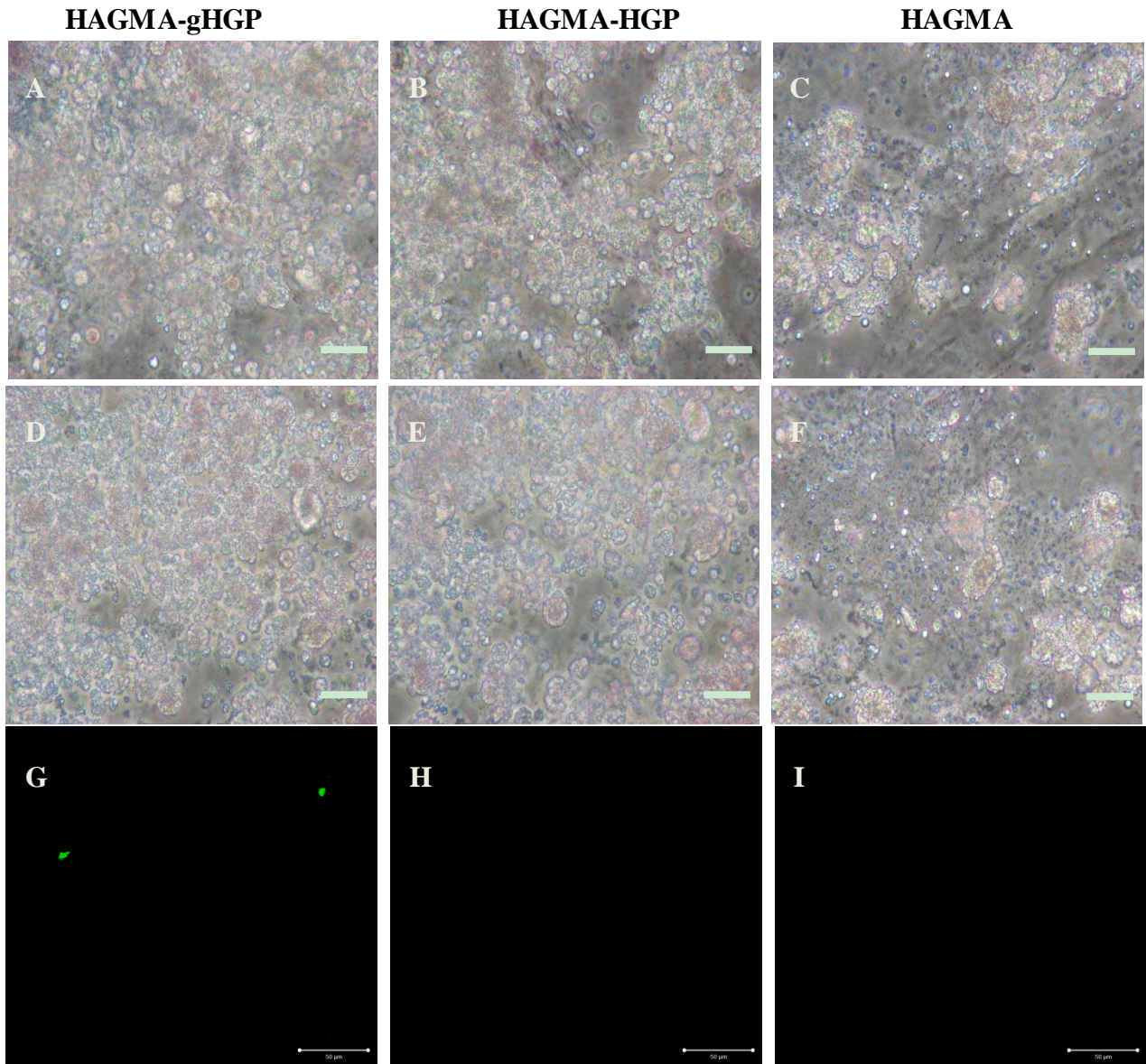


**Figure 3.9** Staining of (A-C) lipids with Oil Red O, (D-F) calcium with Alizarin Red S and (G-I) Collagen I with antibodies for cells after 30 days of MSC culture in gels. Scare bar: 50  $\mu$ m

### 3.3.6. Viscoelastic Properties of the Cell/gel Constructs

Mechanical properties of cell-free hydrogels and cell/gel constructs were analyzed by commercial rheometer and TWA. Both measurements were performed within the linear

viscoelastic region: the applied strain was 0.1% for oscillatory rheological tests, and the imposed rotational angle was  $0.2^\circ$  in the torsional wave experiments. At frequencies of 0.1-10 Hz, the storage and loss modulus for HAGMA gels are frequency-independent (Figure 3.10), confirming the covalent nature of the matrices. The hydrogels exhibited  $G'$  values of approximately two orders of magnitude higher than the corresponding  $G''$  values (Table 3.1), indicating that these gels are highly elastic. HAGMA had an average  $G'$  of  $420 \pm 24$  Pa and  $G''$  of  $3 \pm 2$  Pa; both values are lower than those of the gels with particles entrapped. HAGMA-HGP gels had an average  $G'$  of  $708 \pm 21$  Pa and  $G''$  of  $13 \pm 5$  Pa, while HA GMA-gHGP gels had an average  $G'$  of  $730 \pm 18$  Pa and  $G''$  of  $14 \pm 5$  Pa, which demonstrated the lack of significant difference between moduli of the two gels with particles. The loss moduli of HAGMA-HGP gels as well as HAGMA-gHGP gels were one order of magnitude higher than that of HAGMA.

Compared to cell-free hydrogels, the cell/gel constructs were generally stiffer and more viscous. After 30 days of hMSC culture, when the frequency was lower than 10 Hz, cell-seeded HAGMA had an average value  $G'$  of  $540 \pm 50$  Pa and  $G''$  of  $12 \pm 3$  Pa. Cell-seeded HAGMA-HGP had an average value  $G'$  of  $870 \pm 76$  Pa and  $G''$  of  $28 \pm 7$  Pa. Cell-seeded HAGMA-gHGP had a  $G'$  of average value  $1210 \pm 70$  Pa and  $G''$  of  $42 \pm 18$  Pa.

Under a Previous studies<sup>20, 21</sup> demonstrated the capability of the torsional wave apparatus (TWA) in accurately and reliably determining the viscoelasticity of hydrogel samples at frequencies up to 200 Hz. This technique relies on the analysis of the amplification factor

around the resonance frequency of the hydrogel samples by the use of an optical lever technique combined with linear viscoelastic wave analysis. The representative frequency-dependent amplification factors for the best-fit model, along with the experimental data for three different types of hydrogels, are included in Figure 3.11. Model prediction was based on the average values from three consecutive measurements on each type of gels.

The average storage modulus for HAGMA at a resonance frequency of 30 Hz was  $437 \pm 50$  Pa. This value is not significantly different from that measured at low frequencies (0.1-10 Hz). The average storage modulus for HAGMA-HGP gels increased from  $730 \pm 18$  Pa at low frequencies to  $960 \pm 102$  Pa at a resonance frequency of 50 Hz, while the average storage modulus for HAGMA-HGP gels increased from  $708 \pm 21$  Pa at low frequencies to  $910 \pm 92$  Pa at a resonance frequency of 50 Hz.

Compared with cell-free gels, cell-seeded gels had higher moduli. After 30 days of culture, HAGMA-gHGP/MSC constructs had the highest  $G'$  and  $G''$  values, which were significantly different from that of other two gels. The  $G'$  value of cell-seeded HAGMA-gHGP gels changed from  $1210 \pm 70$  Pa at lower frequencies to  $1502 \pm 220$  Pa at a resonance frequency of 50 Hz. The values were larger than those of cell-seeded HAGMA-HGP gels, which changed from  $870 \pm 76$  Pa at lower frequencies to  $1091 \pm 112$  Pa at higher frequencies. This is probably due to an increase of collagen II, aggrecan and sGAG secreted into the matrices of scaffolding gels.

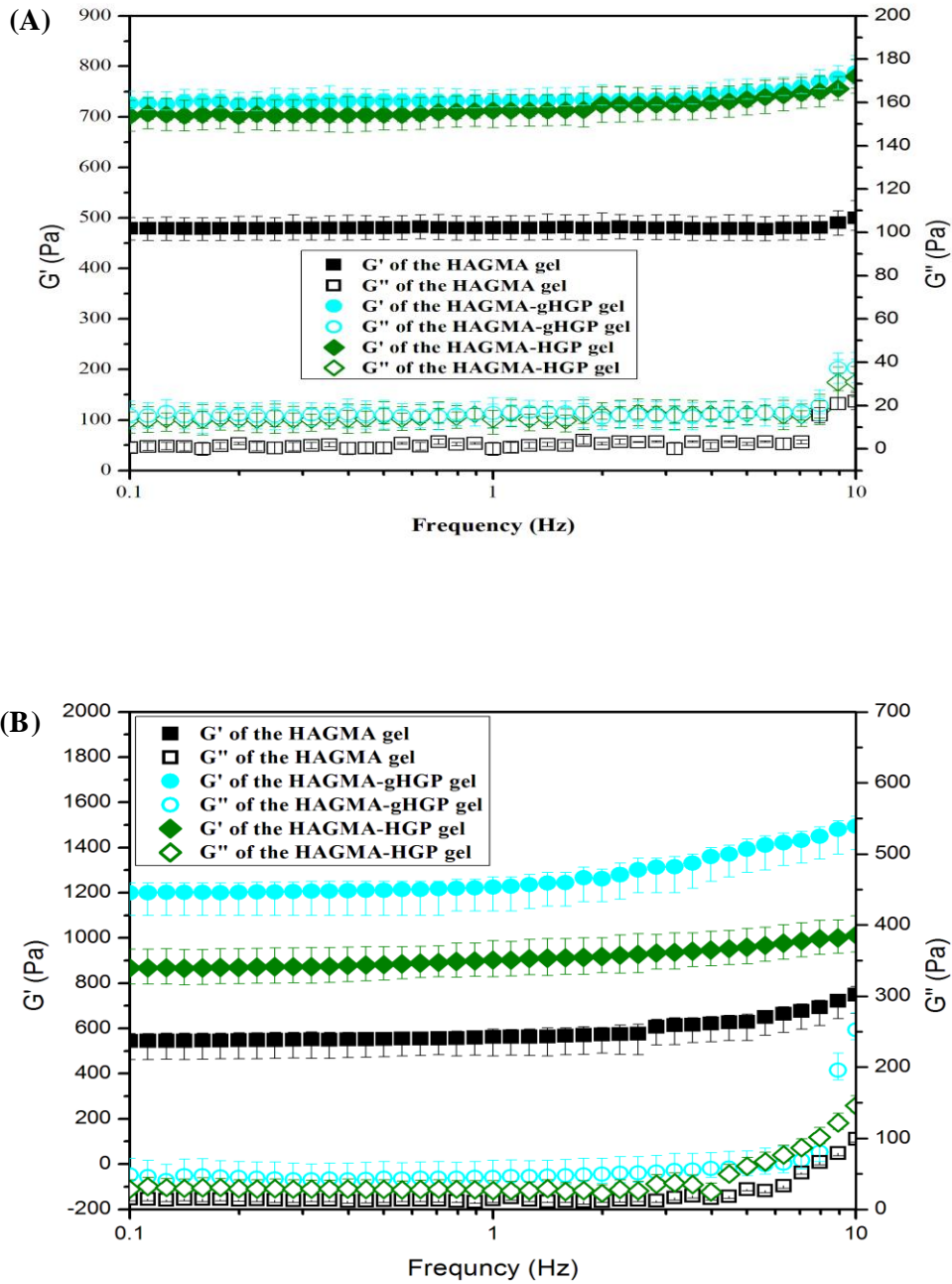


**Figure 3.10** The frequency dependence of the storage (solid symbols) and loss (open symbols) moduli on 0.1% strain for (A) cell-free HA based gels and (B) cell-seeded HA based gels at lower frequency; three repeating samples were used for each type of gels. Cell-seeded gels were removed after 30 days of MSC culture.

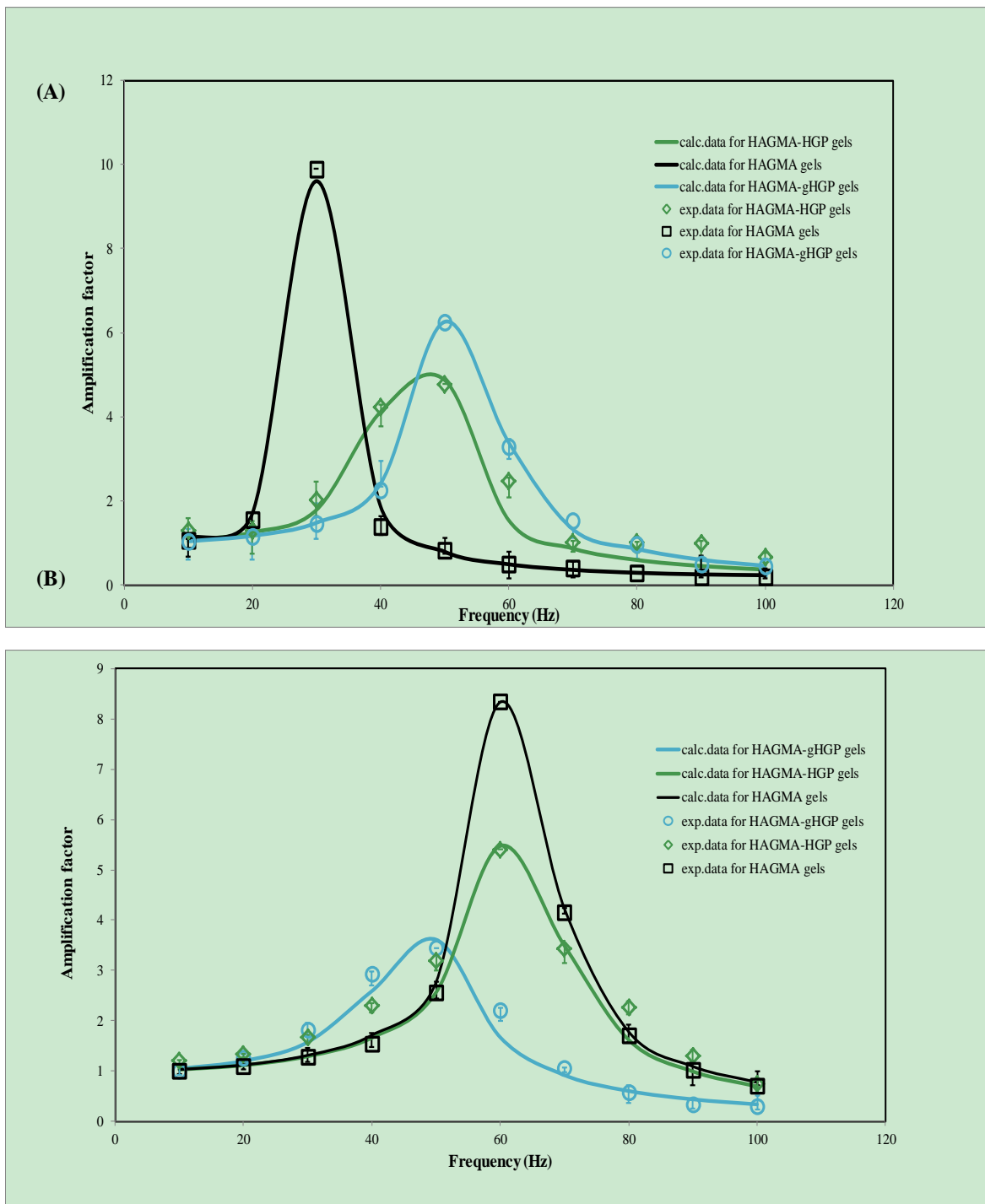


**Figure 3.11** Frequency dependence of amplification factors for (A) cell-free HA based gels and (B) cell seeded gels. The viscoelastic moduli that provide the best fit between model predictions (curves) and experimental results (symbols) for the respective materials were measured. Each experiment was conducted with three repeats.

Samples		0.1-10 Hz		10-100 Hz		
		Average G' (Pa)	Average G''(Pa)	Resonance frequency (Hz)	Average G' (Pa)	Loss tangent tan( $\delta$ )
Cell-free gels	HAGMA gels	480 $\pm$ 24	3 $\pm$ 2	30	437 $\pm$ 50	0.04 $\pm$ 0.01
	HAGMA-gHGP gels	730 $\pm$ 18	14 $\pm$ 5	50	960 $\pm$ 102	0.13 $\pm$ 0.004
	HAGMA-HGP gels	708 $\pm$ 21	13 $\pm$ 5	50	910 $\pm$ 92	0.10 $\pm$ 0.01
Cell-seeded gels	HAGMA gels	540 $\pm$ 50	12 $\pm$ 3	60	642 $\pm$ 70	0.09 $\pm$ 0.01
	HAGMA-gHGP gels	1210 $\pm$ 70	62 $\pm$ 18	50	1502 $\pm$ 220	0.27 $\pm$ 0.02
	HAGMA-HGP gels	870 $\pm$ 76	32 $\pm$ 10	60	1091 $\pm$ 112	0.17 $\pm$ 0.01

**Table 3.1** Viscoelastic properties of HA hydrogels and cell/gel constructs assessed by commercial rheometer at frequencies of 01-10 Hz and TWA at frequencies of 10-100 Hz.

### 3.4. Conclusion

In this chapter, MSCs were cultured in HAGMA gels containing gelatin conjugated HGPs for up to 35 days. Cells remained round shaped and developed focal adhesion in the matrix. Cells in these gels were able to secrete cartilage-specific ECM proteins, such as collagen II, aggrecan, and sGAG. Compared to the cell free matrix, the cell-gel constructs were stiffer and more viscous at the end of 35 days of culture.

## REFERENCES

- [1] Mankin, H. J. *Bone and Joint Surgery* **1982**, *64*, 460–466.
- [2] Xu, J.; Wang, W.; Ludeman, M.; Cheng, K.; Hayami, T.; Lotz, J. C.; Kapila, S. *Tissue Engineering Part A* **2008**, *14*, 667-680.
- [3] Hsu, S. H.; Whu, S. W.; Hsieh, S. C.; Tsai, C. L.; *Artificial Organs* **2004**, *28*, 693-703.
- [4] Park, J. S.; Shim, M. S.; Shim, S. H.; Yang, H. N.; Jeon, S.Y.; Woo, D.G; Lee, D. R.; Yoon, T. K.; Park, K.H. *Biomaterials* **2011**, *32*, 8139-8149.
- [5] Kiliana, K.A.; Bugarija, B.; Lahn, B.T.; Mrksich, M. *Applied Biological Sciences* **2010**, *107*, 4872–4877
- [6] Aulthouse, A. L.; Beck, M.; Griffey, E.; Sanford, J.; Arden, K.; Machado, M. A.; Horton, W. A. *In Vitro Cellular and Developmental Biology* **1989**, *25*, 659-668.
- [7] Kuettner, K. E. *Clinical Biochemistry* **1992**, *25*, 155–163.
- [8] Maheshwari, G; Brown, G; Lauffenburger, D. A.; Wells, A.; Griffith, L. G; *Cell Science* **2000**, *113*,1677-1686.
- [9] Pasirayi, G; Auger, V.; Scott, S. M.; Rahman, P.K.S.M.; Islam, M.; Hare, L.O.; Ali, Z. *Micro and Nanosystems* **2011**, *3*, 137-160
- [10] Xu, X.; Jha, A. K.; Duncan, R. L.; Jia, X. *Acta Biomaterialia* **2011**, *7*, 3050-3059.
- [11] Jha, A. K.; Malik, M. S.; Farach-Carson, M. C.; Duncan, R. L.; Jia, X. *Soft Matter* **2010**, *6*, 5045-5055.
- [12] Jha, A. K.; Yang, W.; Kirn-Safarn, C. B.; Farach-Carson, M. C.; Jia, X. *Biomaterials* **2009**, *30*, 6964-6974.
- [13] Horkay, F.; Basser, P. J.; Hecht, A. M.; Geissler, E. *Chemical Physics* **2008**, *128*, 135103.
- [14] Xu, X.; Jha, A. K.; Harrington, D. A.; Farach-Carson, M. C.; Jia, X. *Soft Matter* **2012**, *8*, 3280-3294.
- [15] Jha, A. K.; Xu, X.; Duncan, R. L.; Jia, X. *Biomaterials* **2011**, *32*, 2466-2478.
- [16] Jia, X.; Burdick, J. A.; Kobler, J.; Clifton, R. J.; Rosowski, J. J.; Zeitels, S. M.; Langer,

- R. Macromolecules* **2004**, *37*, 3239-3248.
- [17] Aeschlimann, P.; Bulpitt, D. J. *Biomedical Materials Research* **1999**, *47*, 152–169.
- [18] Jia, X.; Colombo, G.; Padera, R.; Langer, R.; Kohane, D. S. *Biomaterials* **2004**, *25*, 4797-4804.
- [19] Neuss, S.; Stainforth, R.; Salber, J.; Schenck, P.; Bovi, M.; Knuchel, R.; Perez-Bouza, A. *Cell transplantation* **2008**, *17*, 977-986.
- [20] Clifton, R. J.; Jiao, T.; Bull, C.; *US Patent Application* **2004**, Pub. No. US 2006/0207343 A1.
- [21] Jiao, T.; Farran, A.; Jia, X.; Clifton, R. J. *Experimental Mechanics* **2009**, *49*, 235-246.
- [22] Turley, E. A.; Noble, P. W.; Bourguignon, L. Y. W. *Biological Chemistry* **2002**, *277*, 4589-4592.
- [23] Anderson, S. B.; Lin, C. C.; Kuntzler, D.V.; Anseth, K.S. *Biomaterials* **2011**, *32*, 3564-3574.
- [24] Salinas, C.N.; Anseth, K. S. *Tissue Engineering and Regenerative Medicine* **2008**, *2*, 296–304.
- [25] Grayson, W. L.; Ma, T.; Bunnell, B. *Biotechnology Progress* **2004**, *20*, 905-912.
- [26] Ong S. Y., Dai H., Leong K.W. *Biomaterials* **2006**, *27*, 4087-4097.
- [27] Christley, S.; Alber, M. S.; Newman, S.A. *PLoS Computational Biology* **2007**, *3*, e76.
- [28] Salinas, C. N.; Cole, B. B.; Kasko, A. M.; Anseth, K. S. *Tissue Engineering* **2007**, *13*, 1025-1034.
- [29] Xu, J.; Wang, W.; Ludeman, M.; Cheng, K.; Hayami, T.; Lotz, J. C.; Kapila, S. *Tissue Engineering Part A* **2008**, *14*, 667-680.
- [30] Bhang, S. H.; Jeon, J. Y.; La, W. G.; Seong, J. Y.; Hwang, J. W.; Ryu, S. E.; Kim, B. S. *Biotechnology and Applied Biochemistry* **2011**, *58*, 271-276.
- [31] Daniels, K.; Solorsh, M. *Cell Science* **1991**, *100*, 249-254.
- [32] Yang, F.; Williams, C.G.; Wang, D.A.; Lee, H.; Manson, P. N.; Elisseeff, J. *Biomaterials* **2005**, *26*, 5991-5998.
- [33] Hoshiba, T.; Kawazoe, N.; Chen, G. *Biomaterials* **2012**, *33*, 2025-2031.

## Appendix

### PERMISSION LETTERS

#### Reprint Permission for Figure 1.1

This is a License Agreement between Xinyi Wang ("You") and The IEEE Engineering in Medicine and Biology Society ("IEEE Xplore") provided by Copyright Clearance Center ("CCC"). The license consists of your order details, the terms and conditions provided by Oxford University Press, and the payment terms and conditions.

Confirmation Number	11019893
Order Date	10-Aug-2012
Licensed content publisher	The IEEE Engineering in Medicine and Biology Society
Licensed content publication	IEEE Transactions on Medical Imaging
Licensed content title	LOGISMOS—Layered Optimal Graph Image Segmentation of Multiple Objects and Surfaces: Cartilage Segmentation in the Knee Joint
Licensed content author	Yin Yin
Licensed content date	Dec/2010
Type of Use	Thesis/Dissertation
Institution name	University of Delaware
Title of your work	HYALURONIC ACID-BASED HYDROGELS FOR CARTILAGE REPAIR
Publisher of your work	n/a
Expected publication date	Sep-2012
Permissions cost	34.00 USD
Value added tax	0.00 USD

Total

34.00 USD

[Terms and Conditions](#)